

doi: 10.12029/gc20190320001

李生喜,何碧,杨博,魏志福,陶刚,甘保平,赵飞,孙平原,赵振瑄,黄鹏飞. 2023. 南天山地块塔格拉克地区二长花岗岩锆石 U-Pb 年代学、地球化学特征:对壳源岩浆成因和构造背景的限定[J]. 中国地质, 50(2): 622–639.

Li Shengxi, He Bi, Yang Bo, Wei Zhifu, Tao Gang, Gan Baoping, Zhao Fei, Sun Pingyuan, Zhao Zhenguan, Huang Pengfei. 2023. Zircon U-Pb geochronology and geochemistry of the Tagelake monzogranites in South Tianshan block: Constraints on crustal magmatic origin and tectonic setting[J]. Geology in China, 50(2): 622–639(in Chinese with English abstract).

南天山地块塔格拉克地区二长花岗岩锆石 U-Pb 年代学、地球化学特征:对壳源岩浆成因和构造背景的限定

李生喜¹, 何碧¹, 杨博², 魏志福³, 陶刚⁴, 甘保平⁵, 赵飞¹, 孙平原¹, 赵振瑄¹, 黄鹏飞¹

(1. 甘肃省地质矿产勘查开发局第二地质矿产勘查院,甘肃 兰州 730020;2. 中国地质调查局西安地质调查中心,陕西 西安 710054;3. 中国科学院地质与地球物理研究所兰州油气资源研究中心,甘肃 兰州 730000;4. 西南科技大学环境与资源学院,四川 绵阳 621010;5. 西北大学大陆动力学国家重点实验室,陕西 西安 710069)

提要:【研究目的】西南天山造山带内塔格拉克地区的长条状岩体位于南天山地块,由二长花岗岩组成。厘定该二长花岗岩的形成机制,对南天山壳源岩浆成因的限定、洋盆俯冲消减及碰撞闭合时限等问题的研究具有重要意义。**【研究方法】**本文首次报道了塔格拉克地区二长花岗岩的全岩主量元素、微量元素、锆石 U-Pb 年代学结果。**【研究结果】**LA-ICP-MS 锆石年代学研究揭示出塔格拉克地区二长花岗岩成岩年龄为 $(284.0 \pm 1.9) \sim (284.3 \pm 3.2)$ Ma, 为早二叠世花岗岩。岩石主量元素和微量元素分析结果揭示该二长花岗岩具有 A 型花岗岩特征:(1) SiO_2 ($70.92\% \sim 72.78\%$) 含量高, 碱质 ($\text{K}_2\text{O} + \text{Na}_2\text{O} = 7.91\% \sim 8.44\%$) 含量较高, A/CNK ($0.89 \sim 0.99$) 较高, 表明二长花岗岩为准铝质岩石, 属于高钾钙碱性系列;(2) LREE ($196 \times 10^{-6} \sim 280 \times 10^{-6}$) 相对富集, HREE ($22.8 \times 10^{-6} \sim 28.2 \times 10^{-6}$) 相对亏损, 负 Eu 异常 (δEu 为 $0.51 \sim 0.64$) 明显, 球粒陨石标准化配分模式呈右倾 V 型特征;(3) 富集 Rb、Th 和 K 等大离子亲石元素, 相对亏损 Nb、Ta、Zr、P 和 Ti 等高场强元素。**【结论】**结合区域构造演化,认为塔格拉克地区二长花岗岩形成于后碰撞构造背景。

关 键 词: 锆石 U-Pb 年代学; 地球化学; 二长花岗岩; 地质调查工程; 塔格拉克地区; 南天山地块

创 新 点: 从野外地质特征、岩石地球化学及 LA-ICP-MS 锆石 U-Pb 年代学等方面,查明了南天山地块塔格拉克地区二长花岗岩地球化学特征及其成岩年代,恢复形成时的构造背景,为南天山古洋盆闭合、碰撞造山时限、后碰撞板块构造特征等洋-陆格局的演化等问题提供了新的科学依据。

中图分类号:P581; P597 文献标志码:A 文章编号:1000-3657(2023)02-0622-18

Zircon U-Pb geochronology and geochemistry of the Tagelake monzogranites in South Tianshan block: Constraints on crustal magmatic origin and tectonic setting

LI Shengxi¹, HE Bi¹, YANG Bo², WEI Zhifu³, TAO Gang⁴, GAN Baoping⁵, ZHAO Fei¹, SUN Pingyuan¹, ZHAO Zhenguan¹, HUANG Pengfei¹

(1. The Second Institute of Geology and Minerals Exploration Team, Gansu Provincial Bureau of Geology and Minerals Exploration

收稿日期: 2019-03-20; 改回日期: 2019-10-27

基金项目: 中国地质调查局(12120115021701)资助。

作者简介: 李生喜,男,1986年生,硕士,高级工程师,从事岩石学、地球化学及区域矿产地质研究;E-mail: lishengxidzx@126.com。

and Development, Lanzhou 730020, Gansu, China; 2. Xi'an Center, China Geological Survey, Xi'an 710054, Shaanxi, China; 3. Lanzhou Center for Oil and Gas Resources, Institute of Geology and Geophysics, Chinese Academy of Sciences, Lanzhou 730000, Gansu, China; 4. School of Environment and Resource, Southwest University of Science and Technology, Mianyang 621010, Sichuan, China; 5. State Key Laboratory of Continental Dynamics, Northwest University, Xi'an 710069, Shaanxi, China)

Abstract: This paper is the result of geological survey engineering.

[Objective] The Tagelake strip pluton, outcropped at the south Tianshan terrane in Southwestern Tianshan orogenic belt, is composed of monzogranites. Determining the formation mechanism of the monzogranites has important implications for the crust-derived magma origin and the time limit of subduction and ocean basin closure in South Tianshan Mountains. **[Methods]** In order to determine the formation mechanism of the monzogranites, detailed zircon U-Pb geochronology, major elements and trace elements were firstly conducted. **[Results]** LA-ICP-MS zircon geochronology study reveals that the monzogranites in the Tagelake area crystallized at $(284.0 \pm 1.9) - (284.3 \pm 3.2)$ Ma, indicative of an Early Permian pluton. The results of major elements and trace elements reveal that the monzogranites display the characteristics of A-type granite: (1) The contents of SiO_2 ($70.92\% - 72.78\%$), $\text{K}_2\text{O} + \text{Na}_2\text{O}$ ($7.91\% - 8.44\%$) and A/CNK ($0.89 - 0.99$) are high, indicating that monzogranites are metaluminous rock and belongs to the high potassium calcium alkaline series; (2) The monzogranites are enriched in LREE ($196 \times 10^{-6} - 280 \times 10^{-6}$) and depleted in HREE ($22.8 \times 10^{-6} - 28.2 \times 10^{-6}$). Negative Eu anomaly is obvious, with δEu values of $0.51 - 0.64$, and the monzogranites are characterized by fractionated chondrite-normalized REE patterns; (3) The monzogranites are enriched in Rb, Th, K and other large ion lithophile elements and depleted in Nb, Ta, Zr, P, and other high field strength elements. **[Conclusions]** Combined with the regional tectonic evolution, it is considered that the Tagelake monzogranites were formed in the post-collision tectonic setting.

Key words: zircon U-Pb geochronology; geochemistry; monzogranite; geological survey engineering; Tagelake area; South Tianshan Block

Highlights: On the basis of field geological characteristics, geochemistry with zircon LA-ICP-MS U-Pb dating, we clarified the geochemical characteristics and the formation age, and recovered the formation environment of the monzogranites in Tagelake, south Tianshan terrane. It provides new evidence for the evolution of the ocean basin closure, the time of collision orogeny, and the character of post-collision tectonic setting in the southern Tianshan.

About the first author: LI Shengxi, male, born in 1986, master, senior engineer, engaged in petrology, geochemistry and regional deposit geology research; E-mail: lishengxidzx@126.com.

Fund support: Supported by the project of China Geological Survey (No.12120115021701).

1 引言

天山造山带不仅是中亚造山带的组成部分,也是中国西北部古生代岩浆活动的集中区,并蕴含着丰富的古亚洲洋演化信息(徐学义等,2005;李平等,2018;计文化等,2020),成为近年来研究中亚造山带的形成与演化、陆壳生长和深部组成结构的有利地区之一(秦切,2017;余吉远,2018;耿全如等,2021)。20世纪80年代以来,众多学者对于南天山造山带古生代地质体开展了大量工作,包括高压—超高压变质岩(张立飞等,2005;蒲晓菲,2011;Xiao et al., 2012;郝国杰等,2020;Wu et al., 2021;姜雪薇和吕增,2021)、蛇绿岩发现和研究(刘本培等,1996;李曰俊等,2005)、古生物与地层(Li et al.,

2002;朱永峰等,2005;Qin et al., 2021;王庆同等,2021)、南天山造山带各种构造演化模式(Coleman, 1989;高俊等,2006;Long et al., 2008;Konopelko et al., 2009;黄河等,2011;Huang et al., 2013;周振菊等,2022)、古生代岩浆岩(刘楚雄等,2004;王超等,2007;黄河等,2011;刘春花等,2014;秦切,2017;孟令华等,2022)等。南天山造山带中广泛发育晚古生代侵入体(张招崇等,2009;陈士海等,2020;刘桂萍等,2021),以花岗质侵入岩为主,以闪长质侵入岩、辉长质侵入岩为次(图1)。前人已从南天山造山带晚古生代侵入体的岩石学、地球化学、年代学等方面探讨了南天山的区域构造格局和演化过程(Konopelko et al., 2007, 2009; Long et al., 2008; Huang et al., 2012; Biske et al., 2013;刘春花等,

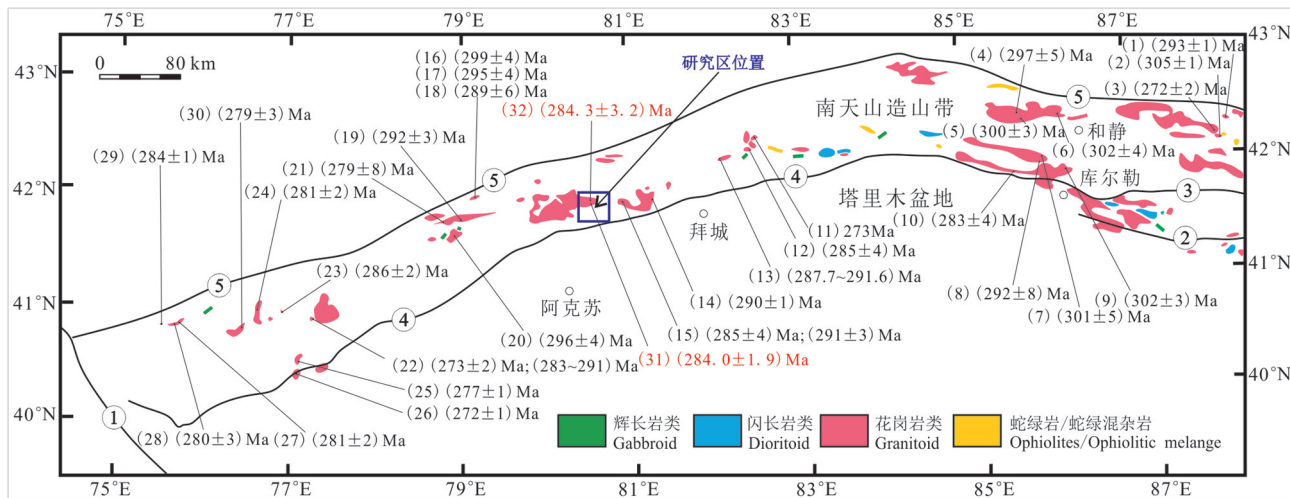


图1 南天山晚古生代侵入岩分布简图(据秦切,2017修改)

①—塔拉斯—费尔干纳右旋走滑断裂;②—兴地断裂;③—辛格尔断裂;④—南天山南缘断裂带;⑤—南天山北缘断裂带

Fig.1 Distribution of the Late Paleozoic intrusive rocks in South Tianshan Mountains (modified from Qin Qie, 2017)

①—Talas—Fergan dextral strike-slip fault; ②—Xingdi fault; ③—Xinggir fault; ④—Fault belt in the southern margin of South Tianshan; ⑤—Fault belt in the northern margin of South Tianshan

2014; Ma et al., 2015; 秦切, 2017)。

但对南天山洋盆俯冲消减及碰撞闭合时限问题仍存争议, 目前不同观点有:早石炭世末、晚石炭世末、中二叠世以前、晚二叠世之后、二叠纪末—三叠纪初等(李曰俊等, 2001; 夏林圻等, 2002; 高俊等, 2006; Zhang et al., 2007; 朱志新等, 2008; Su et al., 2010; Xiao et al., 2013; 毛友亮等, 2014; 黄河等, 2015; 王宗秀等, 2017; 林涛等, 2019; 李智佩等, 2021)。此外, 对南天山后碰撞阶段中酸性岩体的形成过程中是否有幔源物质加入等问题仍未达成共识(黄河等, 2010)。

本文选择南天山塔格拉克地区二长花岗岩为研究对象, 在详细的岩石地球化学及LA-ICP-MS锆石U-Pb年代学研究基础上, 旨在查明其岩石地球化学特征及其成岩年代, 恢复其成岩环境, 为进一步探讨南天山古洋盆闭合、碰撞造山时限、后碰撞板块构造特征等洋-陆格局的演化问题提供新的科学依据。

2 区域地质背景及岩石学特征

塔格拉克地区位于中亚造山带之西天山造山带(图2a), 属于卡拉库姆—塔里木板块(I)、南天山陆块群(II)、木扎尔特陆块(III), 北邻南天山南缘晚古生代弧后盆地, 南邻塔里木盆地(图2b)(王

宗秀等, 2017)。研究区出露的地层有长城系、寒武系、石炭系、二叠系、三叠系、侏罗系、白垩系、古近系、新近系、第四系(图2c), 其中长城系阿克苏群岩性为灰绿色绢云绿泥石英片岩、绿帘绿泥石英片岩、绿泥石英片岩, 寒武系肖尔布拉克组岩性为碳酸盐岩夹少量细碎屑岩, 石炭系阿衣里河组和康克林组岩性为深灰色灰岩夹碎屑岩, 二叠系小提坎立克组岩性为浅灰黑色晶屑凝灰岩、岩屑凝灰岩、英安质晶屑凝灰岩, 三叠系、侏罗系岩性为碎屑岩夹煤层、煤线, 白垩系岩性为碎屑岩, 古近系、新近系岩性为碎屑岩夹石膏层, 第四系岩性为冲积物和冰碛物。研究区火山岩分布较少, 主要分布于二叠系小提坎力克组中, 以中酸性火山碎屑岩为主。研究区出露晚古生代二叠纪岩浆岩(图2c), 属塔吉克—塔里木一级构造岩浆带, 呈巨大的岩基侵入长城系阿克苏群、上石炭统康克林组中, 岩性主要为中粗粒二长花岗岩、粗粒二长花岗岩(图2d)。研究区变质岩主要为区域变质岩, 分布于长城系阿克苏群中, 以石英片岩为主; 在岩体接触带部位, 发育接触变质岩, 岩性为角岩、矽卡岩。研究区区域深大断裂发育, 由中部丹津苏大断裂(F_2)及南部帕喀勒克—提坎库鲁克大断裂(F_3)贯穿整个研究区(图2c)。

塔格拉克地区二长花岗岩, 出露面积约112.9 km²(图2c), 主要位于研究区的北部, 侵入于长城系

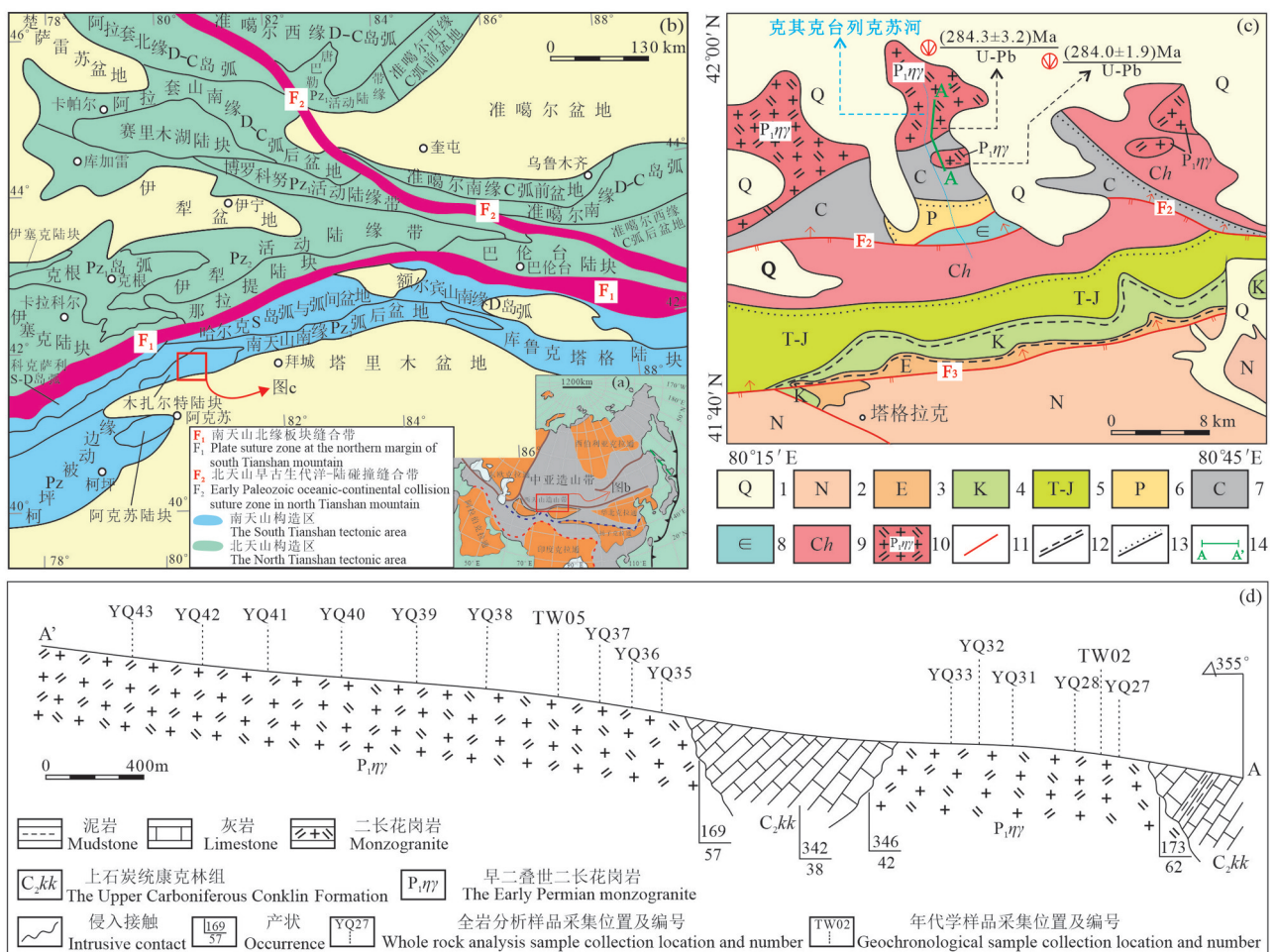


图2 西天山造山带构造单元划分图(a、b,据王宗秀等,2017)和塔格拉克地区地质简图及采样位置图(c、d,据甘肃省地质矿产勘查开发局第二地质矿产勘查院,2018^①)

1—第四系;2—新近系;3—古近系;4—白垩系;5—侏罗系—三叠系;6—二叠系;7—石炭系;8—寒武系;9—长城系;10—早二叠世二长花岗岩;11—断层;12—平行不整合;13—角度不整合;14—剖面位置

Fig.2 Tectonic division in Western Tianshan Orogen (a, b, after Wang Zongxiu et al., 2018) and geological map of Tagelake area with sampling locations (c, d, modified from the Second Institute of Geology and Minerals Exploration Team, Gansu Provincial Bureau of Geology and Minerals Exploration and Development, 2018^①)

1—Quaternary; 2—Neogene; 3—Paleogene; 4—Cretaceous; 5—Jurassic—Triassic; 6—Permian; 7—Carboniferous; 8—Cambrian; 9—Changcheng System; 10—Early Permian monzogranite; 11—Fault; 12—Parallel unconformity; 13—Angular unconformity; 14—Section position

阿克苏群及石炭系中,呈近东西向长条状展布,与围岩接触界线清楚,呈侵入接触。岩石为浅肉红色和浅灰白色,粗中粒结构,块状构造。该二长花岗岩(图3a、b)的主要矿物为斜长石($\pm 40\%$)、钾长石($\pm 35\%$)、石英($\pm 20\%$)、黑云母($\pm 4\%$)、白云母(微)、锆石(微)(图3e)、榍石(微)(图3c)和磷灰石(微)等;斜长石(图3c、d、e、f)呈自形板条状、短柱状和柱粒状,晶体棱边平直,斜长石的自形程度强于钾长石,斜长石晶体为粗中粒级,粒径为2.0~7.0 mm,斜长石发育绢云母化、黏土化、绿帘石化,为

酸性斜长石,见环带构造和聚片双晶;钾长石(图3d、e、f)呈他形粒状,为条纹长石、正长石和微斜长石,条纹长石具条纹结构,微斜长石具格子双晶,微高岭土化,粒径为2.0~6.5 mm;石英(图3c、d、e、f)多为不规则的他形粒状,呈锯齿状镶嵌分布,分布于其他矿物的空隙中,单体粒径相对长石较细小,消光不均匀,单体粒径在5.0 mm以下;暗色矿物为黑云母(图3d、f),部分已绿泥石化,杂乱分布,粒径在0.2 mm×0.5 mm以下;见少量的白云母分布,粒径在0.5 mm以下。

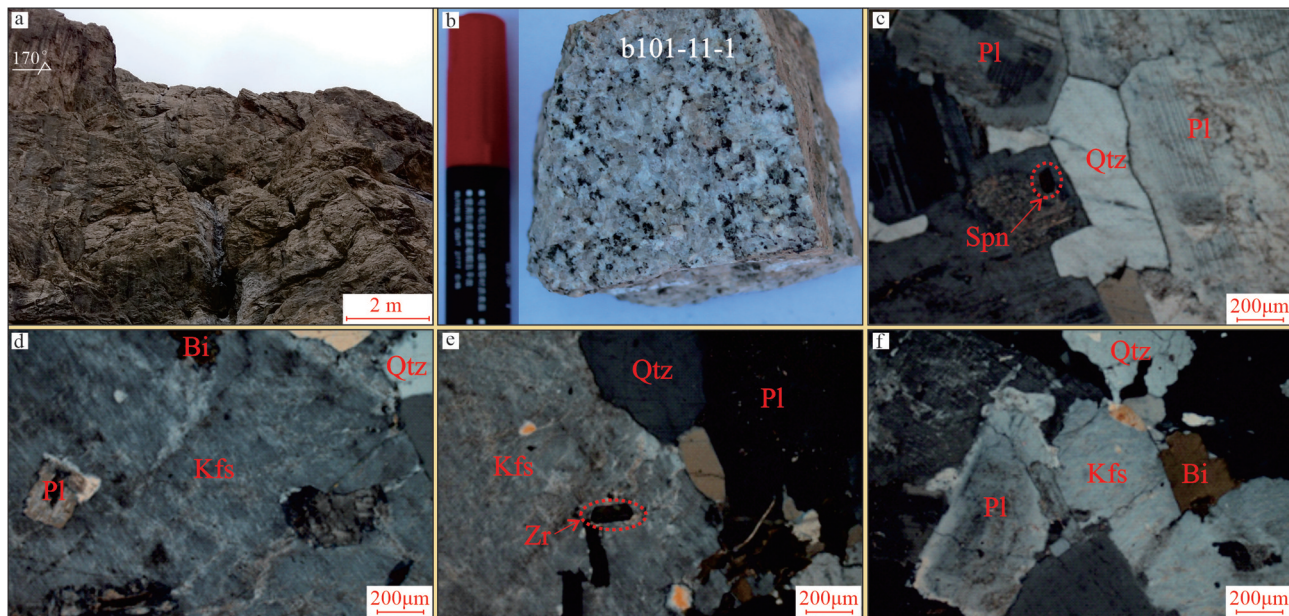


图3 塔格拉克地区二长花岗岩的岩石标本和镜下特征

Qtz—石英; Pl—斜长石; Kfs—钾长石; Bi—黑云母; Zr—锆石; Spn—榍石

Fig.3 Scanned photo of specimens and photomicrographs of the monzogranites in Tagelake area

Qtz—Quartz; Pl—Plagioclase; Kfs—K-feldspar; Bi—Biotite; Zr—Zircon; Spn—Sphene

3 分析方法

为了精确厘定南天山二长花岗岩的形成年代,在塔格拉克地区采集了2件典型的二长花岗岩新鲜样品,采样位置见图2d,样品编号为TW02、TW05,每件重约5 kg,小心排除和避免任何相邻层位和外来物质的污染。从中挑选锆石,经过手工挑选、制靶、剖光和照相观察。锆石的挑选在河北省廊坊市区域地质调查研究所实验室完成,采用标准重矿物技术分选锆石。锆石的制靶、显微镜照相、阴极发光(CL)图像分析在南京聚谱检测科技有限公司完成。将双目镜下挑选的表面平整光洁且具有不同长宽比例、不同柱锥面特征、不同颜色的锆石颗粒粘在双面胶上,用无色透明环氧树脂固定,待固化后对其表面抛光至锆石中心。用反射光和透射光对待测锆石进行照相,然后镀金,进行阴极发光照相,以检查锆石的内部结构和裂隙分布情况,选取锆石U-Pb测试点。本次的锆石测年采用LA-ICP-MS方法,测试工作在南京大学内生金属矿床成矿机制国家重点实验室完成。测试使用与相干193 nm激光取样系统连接起来的Agilent 7500a ICP-MS完成。分析过程中,激光束斑直径

采用32 μm,频率为5 Hz。样品经剥蚀后,由He气作为载气,再和Ar气混合后进入ICP-MS进行分析。U-Pb分馏根据澳大利亚锆石标样GEMOC GJ-1来校正,锆石标样Mud Tank作为内标,控制分析精度;采用专用软件ICP-MS Data Cal完成锆石样品的数据处理工作,包括对样品和空白信号的选择、仪器灵敏度漂移校正、元素含量计算等,并最终给出合理年龄,分析结果见表1。

在塔格拉克地区采集了14件典型的二长花岗岩新鲜样品进行全岩地球化学分析,采样位置见图2d,全岩地球化学分析在华北有色地质勘查局燕郊中心实验室完成。主量元素采用 Axios PW4400型X射线荧光光谱玻璃熔片法分析,稀土元素和微量元素均采用电感耦合等离子体质谱法(ICP-MS)分析,分析结果见表2。

4 锆石U-Pb年龄

2件样品中所挑选的锆石颗粒主要呈自形一半自形棱柱状晶体,长100~300 μm,宽40~100 μm,长宽比在2:1~4:1。研究表明,岩浆成因锆石多具有特征性的韵律环带(Corfu, 2003; 吴元保和郑永飞, 2004; 李长民, 2009),研究区锆石颗粒在CL图像上

表1 塔格拉克地区二长花岗岩LA-ICP-MS锆石U-Pb年龄测定结果

Table 1 LA-ICP-MS U-Pb data of the monzogranites in Tagelake area

测点号	含量/ 10^{-6}			同位素比值						年龄/Ma						
	Pb	Th	U	$^{207}\text{Pb}/^{206}\text{Pb}$		$^{207}\text{Pb}/^{235}\text{U}$		$^{206}\text{Pb}/^{238}\text{U}$		$^{207}\text{Pb}/^{206}\text{Pb}$		$^{207}\text{Pb}/^{235}\text{U}$		$^{206}\text{Pb}/^{238}\text{U}$		
				比值	误差/ 1σ	比值	误差/ 1σ	比值	误差/ 1σ	年龄	误差/ 1σ	年龄	误差/ 1σ	年龄	误差/ 1σ	
TW02-14	36.75	178.14	727.96	0.24	0.0514	0.0007	0.3139	0.0042	0.0442	0.0003	257.5	26.9	277.2	3.3	279.0	1.8
TW02-24	16.57	155.76	307.18	0.51	0.0532	0.0010	0.3254	0.0061	0.0445	0.0003	344.5	44.4	286.0	4.7	280.6	2.1
TW02-12	16.05	127.55	300.86	0.42	0.0516	0.0010	0.3165	0.0063	0.0446	0.0004	264.9	44.4	279.2	4.9	281.4	2.2
TW02-23	10.76	115.16	192.09	0.60	0.0525	0.0011	0.3253	0.0070	0.0450	0.0004	305.6	48.1	286.0	5.4	283.8	2.2
TW02-06	6.35	46.50	119.26	0.39	0.0525	0.0015	0.3233	0.0089	0.0451	0.0004	309.3	64.8	284.5	6.9	284.2	2.6
TW02-18	19.81	217.88	351.22	0.62	0.0523	0.0010	0.3262	0.0061	0.0451	0.0003	298.2	42.6	286.7	4.7	284.4	2.0
TW02-05	22.85	208.86	412.46	0.51	0.0519	0.0008	0.3243	0.0054	0.0453	0.0003	283.4	32.4	285.2	4.1	285.4	1.9
TW02-03	12.35	120.20	221.83	0.54	0.0526	0.0011	0.3275	0.0070	0.0453	0.0004	322.3	48.1	287.6	5.3	285.9	2.2
TW02-01	13.21	89.27	244.98	0.36	0.0528	0.0011	0.3290	0.0067	0.0454	0.0003	320.4	15.7	288.8	5.1	286.1	1.9
TW02-09	15.01	84.08	289.70	0.29	0.0542	0.0012	0.3375	0.0072	0.0456	0.0004	388.9	48.1	295.3	5.5	287.2	2.6
TW02-02	27.68	245.92	495.84	0.50	0.0513	0.0008	0.3228	0.0050	0.0456	0.0003	253.8	39.8	284.1	3.9	287.7	2.0
TW05-18	24.49	289.59	434.43	0.67	0.0516	0.0009	0.3133	0.0051	0.0441	0.0003	333.4	37.0	276.7	4.0	277.9	2.0
TW05-01	37.28	241.70	731.15	0.33	0.0533	0.0007	0.3245	0.0047	0.0441	0.0003	342.7	26.9	285.4	3.6	278.3	2.1
TW05-07	16.84	169.61	307.15	0.55	0.0536	0.0011	0.3267	0.0071	0.0442	0.0003	353.8	80.5	287.0	5.4	278.6	2.0
TW05-24	23.75	249.98	423.78	0.59	0.0520	0.0010	0.3212	0.0065	0.0447	0.0003	283.4	44.4	282.8	5.0	281.9	2.1
TW05-13	27.88	302.37	501.58	0.60	0.0543	0.0009	0.3394	0.0066	0.0450	0.0004	387.1	37.0	296.7	5.0	283.7	2.7
TW05-20	30.29	285.14	547.65	0.52	0.0523	0.0008	0.3253	0.0053	0.0450	0.0003	298.2	41.7	286.0	4.0	284.0	2.0
TW05-19	24.42	255.94	429.96	0.60	0.0527	0.0009	0.3294	0.0057	0.0453	0.0003	322.3	38.9	289.1	4.3	285.5	2.2
TW05-16	29.91	303.99	518.11	0.59	0.0537	0.0008	0.3382	0.0053	0.0456	0.0003	366.7	35.2	295.8	4.0	287.3	1.8
TW05-08	18.47	158.43	335.31	0.47	0.0530	0.0010	0.3333	0.0059	0.0457	0.0003	331.5	36.1	292.1	4.5	288.2	2.0
TW05-02	25.98	212.15	469.51	0.45	0.0528	0.0009	0.3375	0.0061	0.0460	0.0004	320.4	41.7	295.3	4.7	290.2	2.3
TW05-22	28.69	325.85	485.60	0.67	0.0525	0.0008	0.3350	0.0052	0.0462	0.0003	309.3	35.2	293.4	4.0	291.4	2.1

具有明显的岩浆韵律环带(图4);同时,岩浆锆石的Th、U含量较高,且Th/U比值一般大于0.1(Simon and Nigel, 2007),研究区2件样品Th/U比值分别介于0.24~0.62(平均值为0.45)、0.33~0.67(平均值为0.55),均大于0.1,化学成分上也进一步表明锆石均为岩浆成因。TW02样品的11个测点的U-Pb年龄在误差范围内具有较好的一致性,其 $^{206}\text{Pb}/^{238}\text{U}$ 年龄的加权平均年龄为(284.0 ± 1.9)Ma(图4b);TW05样品的11个测点的U-Pb年龄在误差范围内也具有较好的一致性,其 $^{206}\text{Pb}/^{238}\text{U}$ 年龄的加权平均年龄为(284.3 ± 3.2)Ma(图4d)。塔格拉克地区岩体的结晶年龄为(284.0 ± 1.9)~(284.3 ± 3.2)Ma,时代为早二叠世。

5 岩石地球化学

5.1 主量元素

本文在研究区取14个样品进行主量元素分析,结果见表2。二长花岗岩的 SiO_2 含量集中于70.92%~72.78%,平均为71.64%,属酸性岩类(图5a); Al_2O_3 含量在13.12%~14.22%,岩石中碱质含量高, $\text{K}_2\text{O}+\text{Na}_2\text{O}$ 含量为7.91%~8.44%,且 $\text{K}_2\text{O}/\text{Na}_2\text{O}$ 均大于1,相对富钾;相对贫 TiO_2 (0.27%~0.33%)、 MgO (0.26%~

0.37%), MnO (0.04%~0.07%)和 P_2O_5 (0.07%~0.11%)。 TiFe_2O_3 含量在1.19%~5.11%,平均值为2.79%,可能与岩石中黑云母有关。

$\text{SiO}_2-\text{K}_2\text{O}$ 图解(图5b)显示,二长花岗岩样品属于高钾钙碱性系列岩石。二长花岗岩的A/CNK为0.89~0.99,属于准铝质岩石(图5c)。

5.2 稀土元素特征

塔格拉克地区二长花岗岩球粒陨石稀土元素标准化配分图像(图6a)显示,其稀土总量高,在 219×10^{-6} ~ 305×10^{-6} ;轻重稀土分馏明显(LREE/HREE=8.60~11.17, $\text{La}_{\text{N}}/\text{Yb}_{\text{N}}$ =10.08~14.61),轻稀土元素相对富集(LREE= 196×10^{-6} ~ 280×10^{-6}),重稀土元素相对亏损(HREE= 22.8×10^{-6} ~ 28.2×10^{-6}),其配分模式呈右倾V型特征,岩石中 δEu 为0.51~0.64,负Eu异常明显,说明岩浆演化过程中存在一定程度的斜长石的结晶分离或源区斜长石的残留。

5.3 微量元素特征

在原始地幔标准化微量元素蛛网图(图6b)中,二长花岗岩的微量元素变化特征基本一致,样品具有相对一致的配分型式,表明它们在成因上有一定的亲缘关系。样品均表现为富集Rb、Th、K等大离

表2 塔格拉克地区二长花岗岩全岩主量元素(%)和微量元素(10^{-6})组成及有关参数Table 2 Analytical results of major elements (%) and trace elements (10^{-6}) of the monzogranites in Tagelake area

样品编号	YQ27	YQ28	YQ31	YQ32	YQ33	YQ35	YQ36	YQ37	YQ38	YQ39	YQ40	YQ41	YQ42	YQ43						
岩性																				
							二长花岗岩													
SiO ₂	70.92	71.23	72.16	71.02	72.00	72.00	71.12	72.78	72.23	71.03	72.03	71.65	71.02	71.80						
TiO ₂	0.30	0.29	0.31	0.32	0.31	0.29	0.32	0.28	0.27	0.33	0.30	0.27	0.33	0.32						
Al ₂ O ₃	13.12	13.85	13.56	14.22	13.41	13.56	13.85	13.30	13.85	13.89	13.45	13.78	13.92	13.68						
Fe ₂ O ₃	0.44	0.40	0.20	0.44	0.49	0.44	0.24	0.34	0.16	0.69	0.40	0.40	0.40	0.24						
FeO	3.12	2.63	2.72	2.60	2.74	2.45	3.00	2.36	2.36	2.74	2.36	2.36	2.60	2.75						
TFe ₂ O ₃	3.26	2.96	1.48	3.26	3.63	3.26	1.78	2.52	1.19	5.11	2.96	2.96	2.96	1.78						
MnO	0.07	0.05	0.05	0.05	0.05	0.04	0.06	0.05	0.04	0.05	0.05	0.05	0.05	0.05						
MgO	0.32	0.30	0.36	0.35	0.34	0.26	0.33	0.31	0.30	0.34	0.33	0.29	0.37	0.35						
CaO	2.22	2.11	1.85	1.97	1.75	1.80	2.06	1.95	1.90	2.03	1.98	2.00	2.03	1.91						
Na ₂ O	3.27	3.36	3.16	3.30	3.16	3.26	3.36	3.26	3.32	3.36	3.26	3.39	3.59	3.23						
K ₂ O	4.91	4.85	4.75	5.00	5.00	5.01	4.72	4.65	4.78	4.85	4.74	4.92	4.85	4.79						
P ₂ O ₅	0.10	0.07	0.10	0.08	0.09	0.09	0.09	0.07	0.11	0.09	0.09	0.08	0.09	0.09						
LOI	0.94	0.94	0.90	0.68	0.69	0.75	0.88	0.73	0.68	0.61	1.07	0.57	0.74	0.73						
Total	99.73	100.07	100.11	100.03	100.03	99.95	100.03	100.08	100.00	100.01	100.06	99.75	99.98	99.94						
Mg [#]	18.6	19.1	36.2	20.0	17.9	15.7	30.2	22.3	37.1	13.4	20.6	18.6	22.5	31.4						
Na ₂ O+K ₂ O	8.18	8.21	7.91	8.30	8.16	8.27	8.08	7.91	8.10	8.21	8.00	8.31	8.44	8.02						
K ₂ O/Na ₂ O	1.50	1.44	1.50	1.52	1.58	1.54	1.40	1.43	1.44	1.44	1.45	1.45	1.35	1.48						
A/NK	1.23	1.29	1.31	1.31	1.26	1.26	1.30	1.28	1.30	1.29	1.28	1.26	1.25	1.30						
A/CNK	0.89	0.95	0.99	0.99	0.97	0.97	0.96	0.95	0.98	0.96	0.95	0.95	0.94	0.98						
La	57.6	74.6	54.6	63.0	73.5	58.9	70.9	67.0	51.3	49.3	49.6	66.7	75.9	60.9						
Ce	107	129	101	111	127	110	121	122	95.8	91.3	90.2	116	130	110						
Pr	11.9	14.1	11.0	12.4	13.8	12.4	13.6	13.1	10.4	10.0	10.0	12.9	13.9	12.3						
Nd	45.0	49.7	41.2	46.4	48.5	45.4	48.7	47.6	39.0	37.4	38.4	46.6	50.1	46.2						
Sm	8.11	8.74	7.89	8.42	7.84	8.31	8.68	8.83	7.63	7.14	7.11	8.57	8.75	8.36						
Eu	1.45	1.50	1.42	1.54	1.41	1.38	1.46	1.43	1.43	1.35	1.46	1.41	1.42	1.42						
Gd	7.89	7.70	6.82	7.93	7.36	7.90	7.50	7.48	6.46	6.34	6.56	7.18	7.39	7.12						
Tb	1.36	1.30	1.15	1.33	1.19	1.34	1.24	1.27	1.07	1.09	1.13	1.22	1.22	1.18						
Dy	7.22	6.93	6.63	7.53	6.50	7.41	6.69	6.93	6.06	6.03	6.41	6.56	6.44	6.20						
Ho	1.41	1.40	1.32	1.54	1.31	1.52	1.34	1.43	1.26	1.27	1.23	1.34	1.36	1.27						
Er	3.85	3.93	3.79	4.34	3.61	4.23	3.84	4.02	3.57	3.59	3.52	3.76	3.81	3.54						
Tm	0.61	0.62	0.60	0.68	0.58	0.66	0.59	0.65	0.55	0.56	0.56	0.58	0.60	0.52						
Yb	3.85	3.82	3.70	4.24	3.62	3.97	3.76	3.89	3.43	3.51	3.52	3.55	3.73	3.41						
Lu	0.55	0.54	0.52	0.61	0.52	0.57	0.52	0.56	0.49	0.49	0.49	0.51	0.56	0.48						
Y	39.6	38.8	36.5	41.5	35.5	41.5	36.9	38.8	34.0	33.6	36.0	36.0	36.8	34.9						
Rb	185	202	212	213	202	205	204	213	207	196	189	210	201	175						
P	424	286	439	355	399	382	383	325	483	382	401	334	373							
Th	36.0	24.9	20.8	22.1	23.1	21.6	23.8	24.3	19.1	18.2	20.5	24.5	24.2	23.0						
U	6.63	3.87	3.89	4.31	3.29	3.50	3.50	5.43	3.59	3.06	3.89	4.21	4.42	3.75						
K	41260	40614	39742	41778	41783	41924	39521	38853	39951	40505	39750	41179	40568	40081						
Nb	19.5	17.5	18.6	19.0	14.8	18.2	16.2	16.7	16.1	16.2	16.1	16.5	15.5	16.2						
Sr	113	115	114	122	121	99.0	118	118	117	115	117	109	115	118						
Ti	1820	1753	1873	1930	1870	1752	1935	1689	1629	1990	1816	1632	1993	1933						
Ta	1.55	1.74	2.08	1.89	1.35	2.17	1.74	1.92	1.60	1.52	1.56	1.55	1.47	1.42						
Hf	6.09	5.54	5.54	6.35	5.85	6.49	5.27	5.85	4.96	5.45	5.48	5.87	5.57	5.31						
Zr	222	201	196	230	205	231	194	219	181	199	200	214	201	195						
TREE	258	304	241	271	297	264	290	286	228	219	220	277	305	263						
LREE	231	277	217	243	273	237	264	260	205	196	196	252	280	239						
HREE	26.7	26.2	24.5	28.2	24.6	27.6	25.4	26.2	22.8	22.8	23.4	24.7	25.1	23.7						
LREE/HREE	8.65	10.59	8.86	8.64	11.06	8.60	10.39	9.93	8.99	8.60	8.40	10.24	11.17	10.10						
La _n /Yb _n	10.73	14.02	10.59	10.66	14.58	10.65	13.53	12.37	10.74	10.08	10.11	13.48	14.61	12.82						
δEu	0.55	0.55	0.58	0.57	0.56	0.51	0.54	0.52	0.61	0.60	0.64	0.53	0.53	0.55						
δCe	0.95	0.91	0.95	0.92	0.92	0.95	0.89	0.95	0.96	0.95	0.94	0.91	0.91	0.93						
Nb/Ta	12.58	10.09	8.94	10.10	11.02	8.41	9.36	8.70	10.09	10.66	10.35	10.69	10.60	11.41						
La/Nb	2.95	4.25	2.94	3.30	4.94	3.23	4.35	4.01	3.18	3.04	3.07	4.03	4.88	3.76						
Th/Nb	1.85	1.42	1.12	1.16	1.55	1.19	1.46	1.46	1.18	1.12	1.27	1.48	1.56	1.42						
Th/La	0.63	0.33	0.38	0.35	0.31	0.37	0.34	0.36	0.37	0.37	0.41	0.37	0.32	0.38						
Rb/Sr	1.64	1.74	1.85	1.75	1.67	2.07	1.73	1.81	1.76	1.71	1.60	1.92	1.74	1.48						
Rb/Nb	9.49	11.51	11.42	11.17	13.61	11.24	12.54	12.76	12.82	12.11	11.70	12.71	12.94	10.80						
Nb/U	2.94	4.53	4.78	4.43	4.52	5.21	4.65	3.08	4.50	5.29	4.15	3.94	3.52	4.32						
Sm/Nd	0.18	0.18	0.19	0.18	0.16	0.18	0.18	0.19	0.20	0.19	0.18	0.17	0.17	0.18						

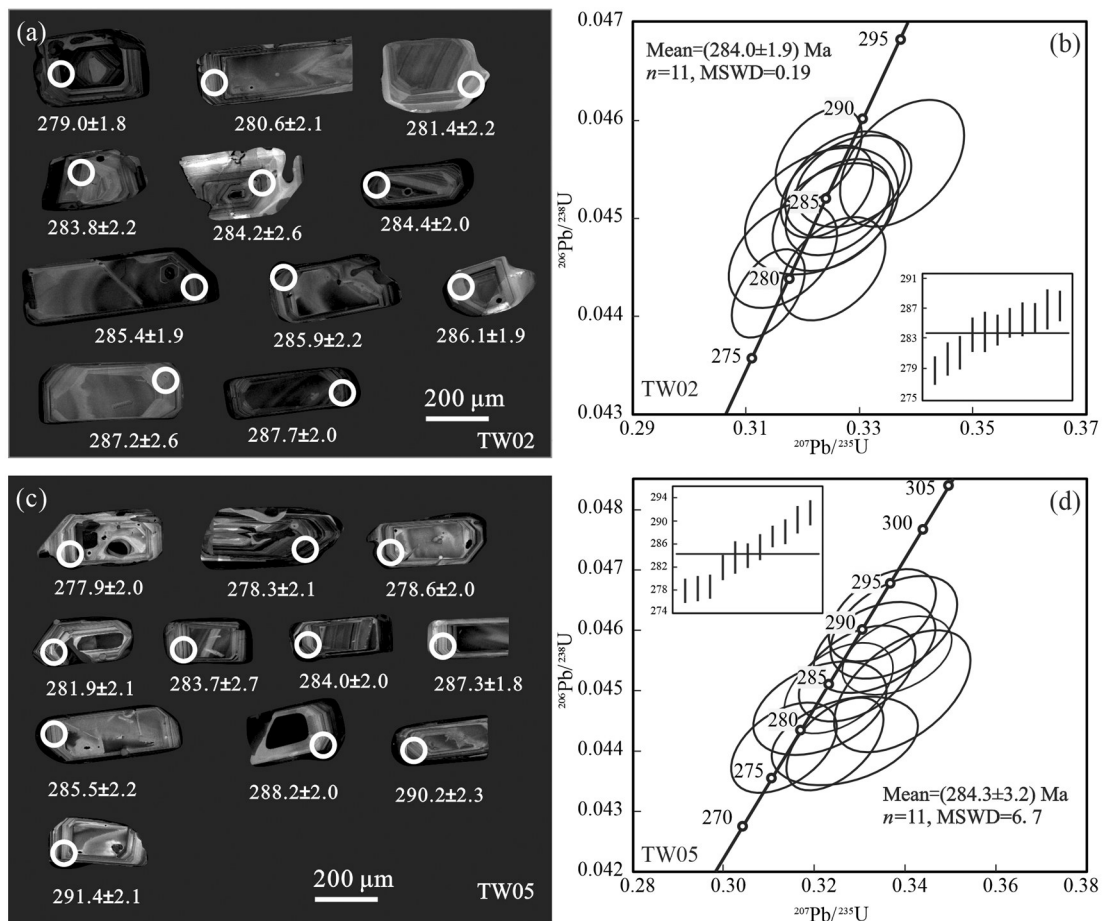


图4 代表性锆石颗粒的CL图像和U-Pb同位素谐和图(a,b为样品TW02,c,d为样品TW05)

Fig.4 Cathodoluminescence images of representative zircon grains and zircon U-Pb isotopic concordia plots for the zircons of sample TW02 (a, b) and TW05 (c, d)

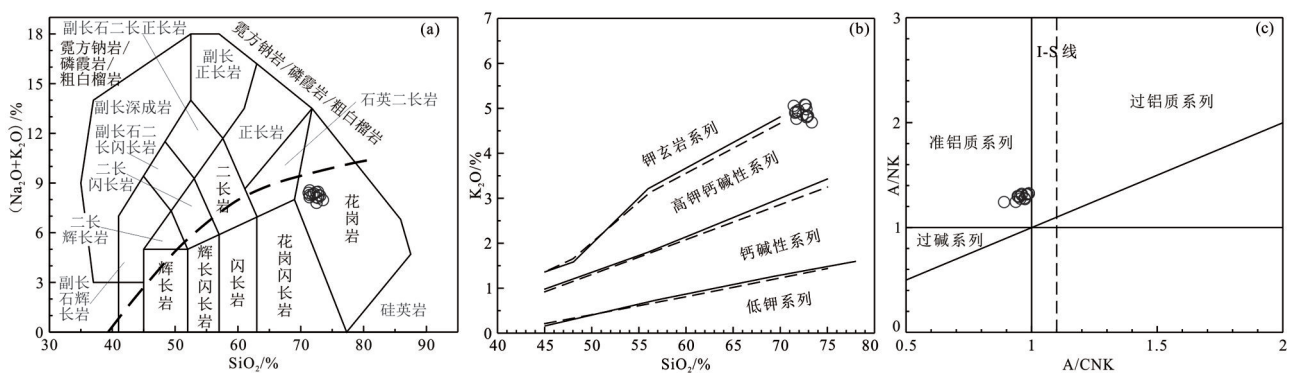


图5 塔格拉克地区二长花岗岩TAS图(a)、SiO₂-K₂O图(b)和A/CNK-A/NK图(c)(a据Mckenzie, 1989; b据Peccerillo and Taylor, 1976; c据Maniar and Piccoli, 1989)

A/CNK—摩尔比[Al₂O₃/(CaO+Na₂O+K₂O)]; A/NK—摩尔比[Al₂O₃/(Na₂O+K₂O)]

Fig.5 TAS (a), SiO₂-K₂O (b) and A/CNK-A/NK (c) diagrams of the monzogranites in Tagelake area (a after Mckenzie, 1989; b after Peccerillo and Taylor, 1976; c after Maniar and Piccoli, 1989)

A/CNK—molar [Al₂O₃/(CaO+Na₂O+K₂O)]; A/NK—molar [Al₂O₃/(Na₂O+K₂O)]

表3 南天山晚古生代花岗质侵入体年代学特征

Table 3 Geochronological data from the granitic plutons at Late Paleozoic in South Tianshan Mountains

岩体编号(图1)	产出位置	岩性	年龄/Ma	数据来源
1	库米什	花岗岩	293±1	黄岗等,2011
2	库米什	花岗岩	305±1	毛友亮等,2014
3	库米什	碱长花岗岩	272±2	Ma et al., 2015
4	盲起苏	花岗闪长岩	297±5	朱志新等,2008
5	盲起苏	二云母二长花岗岩	300±3	秦切,2017
6	盲起苏	花岗闪长岩	302±4	秦切,2017
7	虎拉山	二云母花岗岩	301±5	秦切,2017
8	虎拉山	二云母花岗岩	292±8	秦切,2017
9	七个星	黑云母二长花岗岩	302±3	秦切,2017
10	库尔楚I号	石榴石花岗岩	283±4	秦切,2017
11	依南里克	花岗岩	273	刘楚雄等,2004
12	黑英山	花岗岩	285±4	Long et al., 2008
13	波孜果尔	花岗岩	287.7~291.6	刘春花等,2014
14	波孜果尔	花岗岩	290±1	Huang et al., 2014
15	英买来	花岗岩	285±4; 291±3	马乐天等,2010; 黄河等,2011
16	吉尔吉斯斯坦	花岗岩	299±4	Konopelko et al., 2009
17	吉尔吉斯斯坦	花岗岩	295±4	Konopelko et al., 2009
18	吉尔吉斯斯坦	花岗岩	289±6	Konopelko et al., 2009
19	吉尔吉斯斯坦	花岗岩	292±3	Konopelko et al., 2009
20	吉尔吉斯斯坦	花岗岩	296±4	Konopelko et al., 2007
21	吉尔吉斯斯坦	花岗岩	279±8	Konopelko et al., 2007
22	巴雷公	碱长花岗岩	273±2; 283~291	王超等,2007; 黄河等,2015
23	川乌鲁	二长岩-正长岩	286±2	Huang et al., 2012
24	吉尔吉斯斯坦	花岗岩	281±2	Konopelko et al., 2007
25	古尔拉勒	花岗岩	277±1	Zhang and Zou., 2013
26	克孜勒	黑云母花岗岩	272±1	Zhang and Zou., 2013
27	吉尔吉斯斯坦	花岗岩	281±2	Biske et al., 2013
28	吉尔吉斯斯坦	花岗岩	280±3	Biske et al., 2013
29	吉尔吉斯斯坦	花岗岩	284±1	Biske et al., 2013
30	吉尔吉斯斯坦	花岗岩	279±3	Konopelko et al., 2007
31	塔格拉克	二长花岗岩	284.0±1.9	本文研究
32	塔格拉克	二长花岗岩	284.3±3.2	本文研究

子亲石元素,相对亏损Nb、Ta、Zr、P和Ti等高场强元素。该岩体具明显的负Eu异常,亏损Sr、Ti、P等元素,相对富集Rb、Th、K、Hf等元素。

6 讨 论

6.1 岩体形成时代

随着锆石高精度测年技术的不断发展,南天山地区新涌出了一批可靠的年代学数据资料,特别是南天山地区晚石炭世—中二叠世(峰期年龄284 Ma)岩浆活动规模相对较大(表3),以花岗质侵入

体为主(秦切,2017),如:库尔楚I号岩体(283 Ma,秦切,2017)、波孜果尔岩体(287.7~291.6 Ma,刘春花等,2014)、川乌鲁岩体(286 Ma, Huang et al., 2012)、英买来岩体(285 Ma,黄河等,2011)、巴雷公岩体(273 Ma,王超等,2007)、黑英山岩体(285 Ma, Long et al., 2008)、依南里克岩体(273 Ma,刘楚雄等,2004)、库米什岩体(272~305 Ma,黄岗等,2011;毛友亮等,2014; Ma et al., 2015)、吉尔吉斯斯坦南天山岩体(279~299 Ma, Konopelko et al., 2007, 2009; Biske et al., 2013)等,这些岩体均形成于南天

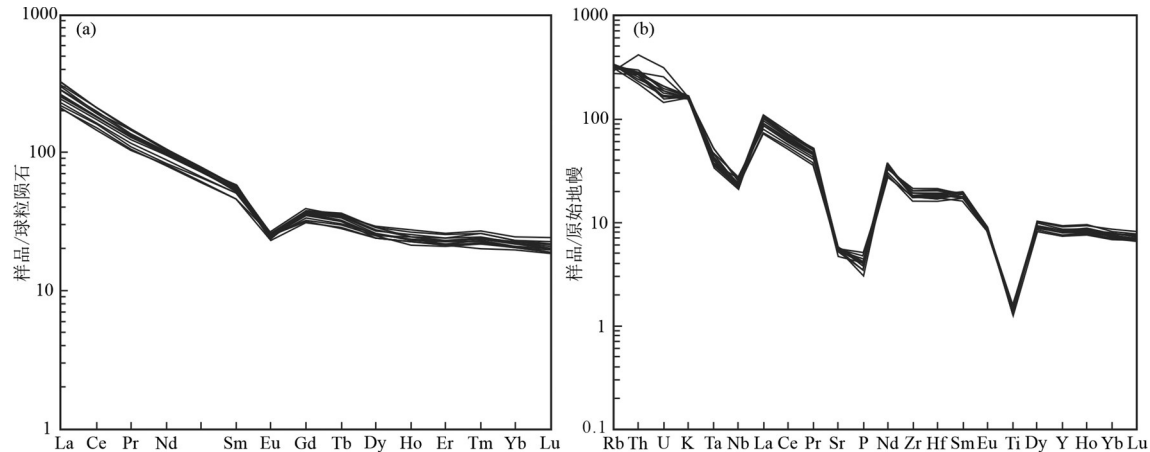


图6 塔格拉克地区二长花岗岩稀土元素球粒陨石标准化配分图(a)与微量元素原始地幔标准化蜘蛛网图(b)(标准化值据Sun and McDonough, 1989)

Fig.6 Chondrite-normalized REE patterns (a) and primitive mantle-normalized trace element spider diagrams (b) of monzogranites in Tagelake area (normalized values are from Sun and McDonough, 1989)

山后碰撞挤压构造背景。本次研究在塔格拉克地区获得2组二长花岗岩的锆石U-Pb年龄分别为 $(284.0\pm1.9)\text{Ma}$ 和 $(284.3\pm3.2)\text{Ma}$,与南天山地区晚石炭世—中二叠世岩浆活动的峰期年龄(284 Ma)高度一致,属于早二叠世。

6.2 岩石成因

关于A型花岗岩的成因主要有以下5种:下地壳岩石的部分熔融和再熔融(Hoskin and Schaltegger, 2003)、幔源拉斑质岩浆高度分异或玄武质岩石部分熔融(Turner et al., 1992;张旗等,2007)、壳幔物质的混合作用(Dickina et al., 1991)、幔源岩浆的分离结晶(Pearce et al., 1984;张旗等,2007)、上地壳钙碱性岩石的低压部分熔融(Spulber and Rutherford, 1983)。因此,A型花岗岩的成因探讨应结合岩体的岩石学、地球化学特征、岩体自身构造和大地构造背景及动力学等多种特征综合分析。

南天山地块塔格拉克地区二长花岗岩具有高硅($70.92\% \sim 72.78\%$)、高碱($\text{K}_2\text{O}+\text{Na}_2\text{O}$ 含量 $7.91\% \sim 8.44\%$)、富铝($13.12\% \sim 14.22\%$)和低 TiO_2 ($0.27\% \sim 0.33\%$)、 MgO ($0.26\% \sim 0.37\%$)、 P_2O_5 ($0.07\% \sim 0.11\%$),属于高钾钙碱性系列。二长花岗岩球粒陨石标准化分布模式呈右倾V型特征,Eu呈明显负异常,轻重稀土分馏程度不高($\text{La}_{\text{N}}/\text{Yb}_{\text{N}}$ 为 $10.08 \sim 14.61$),表现为富集Rb、Th、K等大离子亲石元素,明显亏损高场强元素(Nb、Ta、Ti)及Sr、P的特征,反映了地壳源区特点(Mckenzie, 1989),同时也显示出A型花岗岩

的特征。另外,二长花岗岩A/CNK值范围为 $0.89 \sim 0.99$,表现出准铝质特征,具有高 Fe^* 值($\text{FeO}^T/(\text{FeO}^T+\text{MgO})$, $0.79 \sim 0.93$)和具较高的 TiO_2/MgO 比值($0.86 \sim 1.12$),上述特征与典型A型花岗岩特征一致。在 $(\text{Zr}+\text{Nb}+\text{Ce}+\text{Y})-\text{FeO}^T/\text{MgO}$ 图解(图7a)及 $(\text{Zr}+\text{Nb}+\text{Ce}+\text{Y})-(\text{Na}_2\text{O}+\text{K}_2\text{O})/\text{CaO}$ 图解(图7b)中,几乎所有样品落于分界线上或A型花岗岩区域,落入分界线上的样品可能是由于分异程度较高导致 Zr 含量的明显降低引起的(Waston and Harrison, 1983);在 $\text{K}_2\text{O}-\text{Na}_2\text{O}$ 图解上(图7c),所有样品落于A型花岗岩区域;由于微量元素易受结晶分异的影响,Frost et al.(2001)提出新的判别图解,在 $\text{SiO}_2-\text{FeO}^T/(\text{FeO}^T+\text{MgO})$ 图解中(图8a)和 $\text{SiO}_2-(\text{Na}_2\text{O}+\text{K}_2\text{O}-\text{CaO})$ 图解中(图8b)中,所有样品均落于A型花岗岩区域。综上所述,南天山地块塔格拉克地区二长花岗岩应属于A型花岗岩。

研究表明:Ta和Nb为强不相容元素, Nb/Ta 比值在岩浆分异中不会造成较大的分异,因此,能够指示岩浆源区特征及演化过程(Green, 1995)。研究区14件二长花岗岩样品 Nb/Ta 比值为 $8.41 \sim 12.58$ (壳源岩浆的 Nb/Ta 比值为 $11 \sim 12$,幔源岩浆的 Nb/Ta 比值为 17.5 ± 2 (Green, 1995)),暗示岩浆的壳源属性; La/Nb 比值为 $2.94 \sim 4.94$,均大于1,表明岩石也源于壳源(Depaolo and Daley, 2000);MORB(洋中脊玄武岩)和OIB(洋岛玄武岩)中 Nb/U 比值为 47 ± 10 ,原始地幔中 Nb/U 平均比值为33.59,但大陆

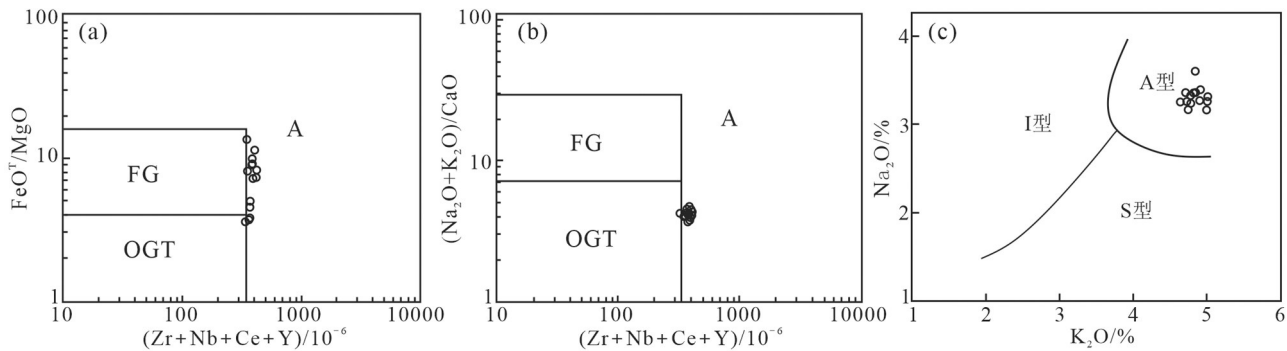


图7 塔格拉克地区二长花岗岩的 $(\text{Zr}+\text{Nb}+\text{Ce}+\text{Y})-\text{FeO}^{\text{T}}/\text{MgO}$ 图、 $(\text{Zr}+\text{Nb}+\text{Ce}+\text{Y})-(\text{K}_2\text{O}+\text{Na}_2\text{O})/\text{CaO}$ 图和 $\text{K}_2\text{O}-\text{Na}_2\text{O}$ 图(a, b据 Whalen et al., 1987; c据 Zorpi et al., 1989)

A—A型花岗岩；FG—分异型I、S或M型花岗岩；OGT—未分异的I、S或M型花岗岩

Fig.7 $(\text{Zr}+\text{Nb}+\text{Ce}+\text{Y})-\text{FeO}^{\text{T}}/\text{MgO}$ (a), $(\text{Zr}+\text{Nb}+\text{Ce}+\text{Y})-(\text{K}_2\text{O}+\text{Na}_2\text{O})/\text{CaO}$ (b) and $\text{K}_2\text{O}-\text{Na}_2\text{O}$ diagrams (c) of the monzogranites in Tagelake area (a, b after Whalen et al., 1987; c after Zorpi et al., 1989)

A—A-type granites; FG—Fractionated M-, I- and S-type granites; OGT—Unfractionated M-, I- and S-type granites

地壳中该比值很低(Taylor and McLennan, 1985),研究区二长花岗岩低的Nb/U值(2.94~5.29),远低于前两者比值;此外,研究区样品Sm/Nd比值在0.16~0.20,与大陆地壳的Sm/Nd比值(0.17~0.25)相近,反映岩石组分多源于地壳(陈加杰等,2016)。综上所述,塔格拉克地区二长花岗岩的微量元素特征显示出壳源属性。

研究区岩体缺乏详细的Sr-Nd同位素资料,导致不能对塔格拉克地区二长花岗岩的源岩或成因模式进行准确的限制;另外,塔格拉克地区二长花岗岩周围并不存在同期玄武质岩石密切共生,因此,认为其不可能由地幔玄武质岩浆高度结晶分异形成。岩体具有较高的 SiO_2 (70.92%~72.78%)和 K_2O (4.65%~5%)含量及较低的 $\text{Mg}^{\#}$ (13.4~37.1),这些特征基本排除了幔源或壳幔混合成因,而暗示岩体可能起源于古老地壳物质的重融。此外,研究区岩体亏损Nb,进一步表明不可能由地幔基性岩浆结晶分异形成(Green, 1995; 杨高学等,2013)。在早二叠世时期,南天山已经进入碰撞后伸展阶段(夏林圻等,2004),塔格拉克地区二长花岗岩可能是在早二叠世后碰撞岩石圈伸展背景下形成。

6.3 构造背景及地质意义

区域地质资料已表明,南天山洋闭合时间不晚于晚石炭世,且在290 Ma已经处于岩石圈伸展背景下后碰撞演化阶段(Chen et al., 1999; 夏林圻等,2004; 刘楚雄等,2004; 高俊等,2006; 黄河等,2011; 刘春花等,2014; 林涛等,2019)。杨蓉(2016)研究

认为早二叠世大量A型花岗岩的涌现揭示晚石炭世—早二叠世西天山地区已进入后碰撞晚期向伸展环境的转化阶段;秦切(2017)认为晚石炭世南天山地区已进入后碰撞环境;刘楚雄等(2004)研究认为塔里木北缘南天山一带的碱性侵入岩(黑英山克其克果勒霓霞正长岩锆石U-Pb年龄275 Ma、依南里克黑云霞石歪长伟晶岩锆石U-Pb年龄273 Ma)形成于后造山的拉张构造环境;吉尔吉斯南天山地区碱性花岗岩(280~266 Ma)形成于后碰撞构造(Solomovich and Trifonov, 2002);高俊等(2006)在研究南天山造山带的花岗岩类、蛇绿岩、高压变质岩等方面的成果基础上,认为南天山洋在早石炭世闭合,南天山西段造山带(塔里木地块与伊犁地块)开始于早石炭世(345 Ma),结束于晚石炭世末(~300 Ma)(Allen et al., 1993; Carroll et al., 1995; Gao et al., 1998; 高俊等,2006);刘春花等(2014)研究南天山拜城县波孜果尔A型花岗岩类(287.7~291.6 Ma)认为南天山古洋盆闭合(碰撞造山)最晚发生在晚石炭世,早二叠世已经进入后碰撞演化阶段。

区域上,大哈拉军山组岛弧型火山岩的最年轻年龄为313 Ma(朱永峰等,2005)、后碰撞火山浅侵位岩浆岩Ar-Ar年龄306~250 Ma(赵振华等,2003),进一步说明南天山碰撞造山事件在石炭纪末结束;塔里木地块和伊犁地块的古地磁特征显示早二叠世时期塔里木地块与伊犁地块已联合为一整体(蔡东升等,1995; 贾承造,1997; Chen et al., 1999),表明天山的碰撞造山结束时间应早于二叠纪;库车盆

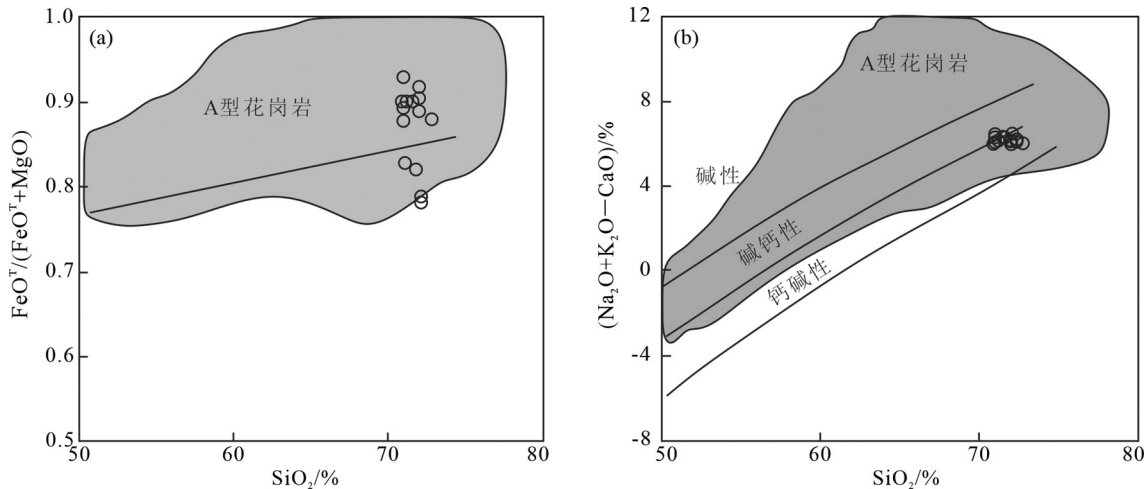


图8 塔格拉克地区二长花岗岩的 $\text{SiO}_2-\text{FeOT}/(\text{FeOT}+\text{MgO})$ 图和 $\text{SiO}_2-(\text{Na}_2\text{O}+\text{K}_2\text{O}-\text{CaO})$ 图(据Frost et al., 2001)
Fig.8 $\text{SiO}_2-\text{FeOT}/(\text{FeOT}+\text{MgO})$ and $\text{SiO}_2-(\text{Na}_2\text{O}+\text{K}_2\text{O}-\text{CaO})$ diagrams of the monzogranites in Tagelake area (after Frost et al., 2001)

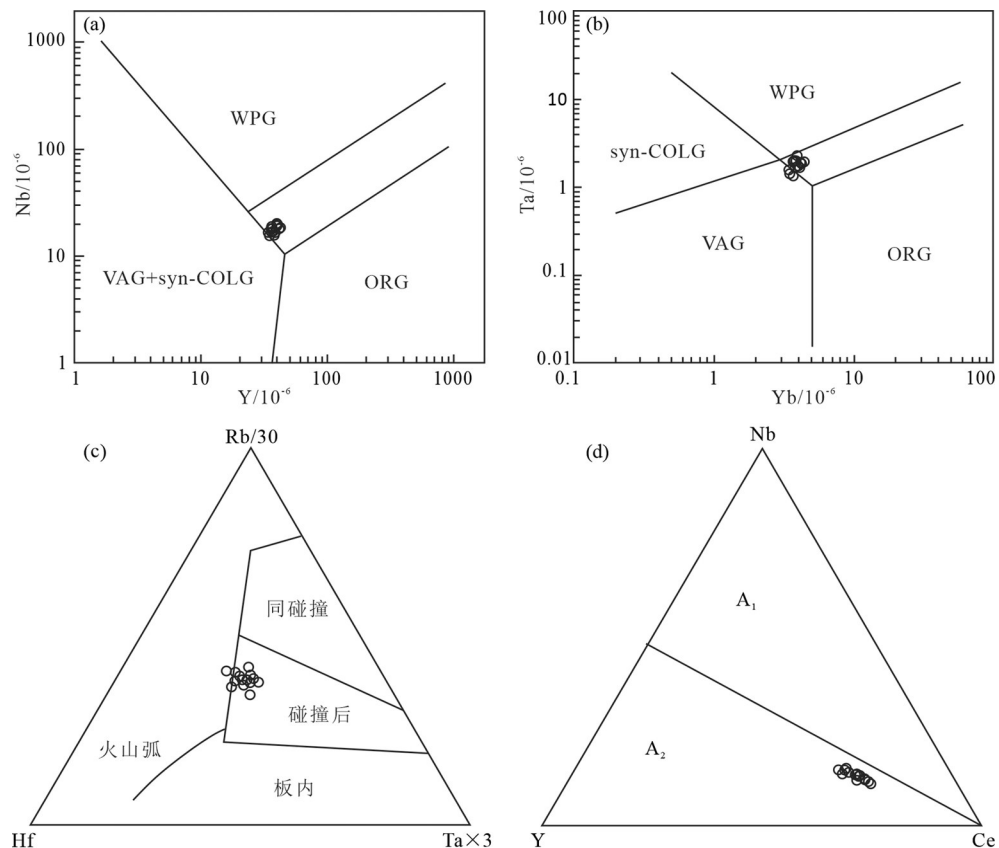


图9 塔格拉克地区二长花岗岩的Y-Nb图(a)、Yb-Ta图(b)、Rb/30-Hf-Ta×3图(c)与Nb-Y-Ce图(d)(a, b after Pearce et al., 1984; c after Harris et al., 1986; d after Eby, 1992)
syn-COLG—同碰撞型; VAG—火山弧型; WPG—板内型; ORG—洋中脊型; A_1 —非造山A型花岗岩; A_2 —造山后A型花岗岩
Fig.9 Y-Nb (a), Yb-Ta (b), Rb/30-Hf-Ta×3 (c) and Nb-Y-Ce (d) diagrams of the monzogranites in Tagelake area (a, b after Pearce et al., 1984; c after Harris et al., 1986; d after Eby, 1992)
syn-COLG—syn-collision granite; VAG—Volcanic arc granite; WPG—Within plate granite; ORG—Oceanic ridge granite; A_1 —Anorogenic A-type granitoids; A_2 —Orogenic A-type granitoids

地的沉积地层序列特征揭示了上二叠统比尤勒包谷孜组陆相磨拉石沉积(周宗良等,1999),也指示了南天山造山带为一晚古生代造山带。

南天山塔格拉克地区二长花岗岩富钾(K_2O 为4.65%~5.01%),体现出碰撞后的A型花岗岩特征(张旗等,2012;赵闯等,2021;赵亚云等,2022),A型花岗岩形成于地壳减薄环境,出现在碰撞后和板内构造背景(徐学义等,2005;张旗等,2012)。在 $Y-Nb$ 和 $Yb-Ta$ 图解中(图9a、b),几乎所有样品均投入板内花岗岩环境区域,反映了碰撞后的岩浆生成环境;在 $Rb/30-Hf-Ta \times 3$ 图解中(图9c),几乎全部样品投入碰撞后区域,也体现了碰撞后的构造背景;在 $Nb-Y-Ce$ 图解上(图9d),样品全部投入A2型花岗岩区域,同样体现出了碰撞后的构造背景,表明花岗岩岩浆起源于地壳(Eby,1992),产于碰撞后的张性构造环境。

综合上述分析,结合区域构造演化,认为塔格拉克地区二长花岗岩(~284 Ma)属于塔里木板块与伊犁板块碰撞后岩石圈伸展背景下的产物,进一步表明南天山塔格拉克地区在早二叠世时期已经进入后碰撞演化阶段,南天山古洋盆闭合(碰撞造山)在早二叠世之前已结束。

7 结 论

通过对南天山地块塔格拉克地区岩体野外地质调查、岩相学、岩石地球化学和锆石U-Pb年代学研究,得出如下结论。

(1)本文获得塔格拉克地区岩体中锆石岩浆振荡环带的LA-ICP-MS U-Pb年龄分别为 (284.0 ± 1.9) Ma、 (284.3 ± 3.2) Ma,属于早二叠世岩浆活动产物,与南天山地块大量早二叠世岩浆活动时间一致。

(2)塔格拉克地区岩体岩性为二长花岗岩, SiO_2 、碱质含量较高,相对富钾,准铝质岩石,属于高钾钙碱性系列,具有高的 Fe^* 值和 TiO_2/MgO 比值;富集轻稀土,亏损重稀土,负Eu异常明显,球粒陨石标准化配分模式呈右倾V型特征;富集Rb、Th、K等大离子亲石元素,相对亏损Nb、Ta、Zr、P和Ti等高场强元素,分析表明二长花岗岩具有壳源属性,属于A型花岗岩。

(3)结合区域构造演化,认为塔格拉克地区二

长花岗岩形成于塔里木板块与伊犁板块碰撞后的岩石圈伸展背景。

致谢:感谢项目组成员在野外样品采集过程中的大力帮助,以及编辑和两位匿名审稿人认真评阅稿件,并提出许多宝贵意见。

注释

①甘肃省地质矿产勘查开发局第二地质矿产勘查院. 2018. 新疆拜城县塔格拉克—关其特一带铜多金属矿远景调查报告[R]. 94-115.

References

- Allen M B, Windley B F, Zhang C. 1993. Palaeozoic collisional tectonics and magmatism of the Chinese Tien Shan, central Asia[J]. Tectonophysics, 220(1/4): 89–115.
- Biske Y S, Konopelko D L, Seltmann R. 2013. Geodynamics of Late Paleozoic magmatism in the Tian Shan and its framework[J]. Geotectonics, 47(4): 291–309.
- Cai Dongsheng, Lu Huafu, Jia Dong, Wu Shimin. 1995. Paleozoic plate tectonic evolution of southern Tianshan[J]. Geological Review, 41(5): 432–443 (in Chinese with English abstract).
- Carroll A R, Graham S A, Hendrix M S, Ying D, Zhou D. 1995. Late Paleozoic tectonic amalgamation of northwestern China: Sedimentary record of the northern Tarim, northwestern Turpan, and southern Junggar basins[J]. Geological Society of America Bulletin, 107(5): 571–594.
- Chen C, Lu F, Jia D, Cai D, Wu S. 1999. Closing history of the southern Tianshan oceanic basin, Western China: An oblique collisional orogeny[J]. Tectonophysics, 302: 23–40.
- Chen Jiajie, Fu Lebing, Wei Junhao, Tian Ning, Xiong Le, Zhao Yujing, Zhang Yujie, Qi Yueqing. 2016. Geochemical characteristics of late Ordovician granodiorite in Gouli Area, Eastern Kunlun Organic Belt, Qinghai Province: Implications on the evolution of Proto-Tethys Ocean[J]. Earth Science, 41(11): 1863–1882 (in Chinese with English abstract).
- Chen Shihai, Zhong Wen, Zhang Jianren. 2020. Geochronology and geochemistry of the Jinghan granitic pluton in South Tianshan, Xinjiang and their tectonic significance[J]. East China Geology, 41(2): 128–141 (in Chinese with English abstract).
- Coleman R G. 1989. Continental growth of northwest China[J]. Tectonics, 8: 621–635.
- Corfu F. 2003. Atlas of zircon textures[J]. Reviews in Mineralogy and Geochemistry, 53: 469–495.
- Depaolo D J, Daley E E. 2000. Neodymium isotopes in basalts of the southwest basin and range and lithospheric thinning during continental extension[J]. Chemical Geology, 169(1): 157–185.
- Dickina A P, Halliday A N, Bowden P A. 1991. Pb, Sr and Nd isotope

- study of the basement and Mesozoic ring complexes of the Jos Plateau, Nigeria[J]. *Chemical Geology: Isotope Geoscience Section*, 94(1): 23–32.
- Eby G N. 1992. Chemical subdivision of the A-type granitoids: Petrogenetic and tectonic implications[J]. *Geology*, 20(7): 641–644.
- Frost B R, Barnes C G, Frost C D. 2001. A geochemical classification for granitic rocks[J]. *Journal of Petrology*, 42: 2033–2048.
- Gao J, Li M S, Tang Y Q, He G Q. 1998. Paleozoic tectonic evolution of the Tianshan Orogen, northwestern China[J]. *Tectonophysics*, 287(1/4): 213–231.
- Gao Jun, Long Lingli, Qian Qing, Huang Dezhi, Su Wen, Klemd R. 2006. South Tianshan: A Late Paleozoic or a Triassic orogen?[J]. *Acta Petrologica Sinica*, 22(5): 1049–1061 (in Chinese with English abstract).
- Geng Quanru, Li Wenchang, Wang Liqian, Zeng Xiangting, Peng Zhimin, Zhang Xiangfei, Zhang Zhang, Cong Feng, Guan Junlei. 2021. Paleozoic tectonic framework and evolution of the central and western Tethys[J]. *Sedimentary Geology and Tethyan Geology*, 41(2): 297–315 (in Chinese with English abstract).
- Green T H. 1995. Significance of Nb/Ta as an indicator of geochemical processes in the crust–mantle system[J]. *Chemical Geology*, 120(3/4): 347–359.
- Hao Guojie, Wang Huichu, Niu Guanghua, Kang Jianli, Hao Shuang. 2020. Metamorphic geotectonic research and scientific significance in China[J]. *Geological Survey and Research*, 43(2): 89–96 (in Chinese with English abstract).
- Harris N B W, Pearce J A, Tindle A G. 1986. Geochemical characteristics of collision–zone magmatism, collision tectonics[J]. *Geological Society of London Special Publications*, 19(1): 67–81.
- Hoskin P W O, Schaltegger U. 2003. The composition of zircon and igneous and metamorphic petrogenesis[J]. *Reviews in Mineralogy and Geochemistry*, 53(1): 27–62.
- Huang Gang, Zhang Zhanwu, Dong Zhihui, Zhang Wenfeng. 2011. Zircon LA–ICP–MS U–Pb age of plagiogranite from Tonghuashan ophiolite in Southern Tianshan mountains and its geological implications[J]. *Geology in China*, 38(1): 94–102 (in Chinese with English abstract).
- Huang H, Zhang Z C, Kusky T, Santosh M, Zhang S, Zhang D Y, Liu J L, Zhao Z D. 2012. Continental vertical growth in the transitional zone between South Tianshan and Tarim, western Xinjiang, NW China: Insight from the Permian Halajun A1-type granitic magmatism[J]. *Lithos*, 155: 49–66.
- Huang H, Zhang Z, Santosh M, Zhang D Y. 2014. Geochronology, geochemistry and metallogenetic implications of the Bozigu'er rare metal–bearing peralkaline granitic intrusion in South Tianshan, NW China[J]. *Ore Geology Reviews*, 61: 157–174.
- Huang H, Zhang Z, Santosh M, Zhang D Y, Zhao Z D, Liu J L. 2013. Early Paleozoic tectonic evolution of the South Tianshan Collisional Belt: Evidence from geochemistry and zircon U–Pb geochronology of the Tiereke Monzonite Pluton, Northwest China[J]. *The Journal of Geology*, 121(4): 401–424.
- Huang He, Wang Tao, Qin Qie, Tong Ying, Guo Lei, Zhang Lei, Hou Jiayao, Song Peng. 2015. Geochronology and zircon Hf isotope of Baleigong granitic pluton in the western part of the South Tianshan Mountains: Petrogenesis and implications for tectonic evolution[J]. *Acta Petrologica et Mineralogica*, 34(6): 971–990 (in Chinese with English abstract).
- Huang He, Zhang Dongyang, Zhang Zhaochong, Zhang Shu, Li Hongbo, Xue Chunji. 2010. Petrology and geochemistry of the Chuanwulu alkaline complex in South Tianshan: Constraints on petrogenesis and tectonic setting[J]. *Acta Petrologica Sinica*, 26(3): 947–962 (in Chinese with English abstract).
- Huang He, Zhang Zhaochong, Zhang Dongyang, Du Hongxing, Ma Letian, Kang Jianli, Xue Chunji. 2011. Petrogenesis of late Carboniferous to early Permian granitoid plutons in the Chinese South Tianshan: Implications for crustal accretion[J]. *Acta Geologica Sinica*, 85(8): 1305–1333 (in Chinese with English abstract).
- Ji Wenhua, Li Rongshe, Chen Fenning, Yang Bo. 2020. Tectonic reconstruction of northwest China in the Nanhai–Paleozoic and discussions on key issues[J]. *Journal of Geomechanics*, 26(5): 634–655 (in Chinese with English abstract).
- Jia Chenzao. 1997. *Tectonic Characteristics and Petroleum, Tarim Basin, China*[M]. Beijing: Petroleum Industry Press, 1–295 (in Chinese with English abstract).
- Jiang Xuewei, Lü Zeng. 2021. Internal structure of deeply subducted accretionary complex in southwestern Tianshan: Implications from the Muzhaerte section[J]. *Acta Petrologica et Mineralogica*, 40(6): 1181–1187 (in Chinese with English abstract).
- Konopelko D, Biske G, Seltmann R, Eklun O, Belyatsky B. 2007. Hercynian post–collisional A-type granites of the Kokshaal Range, Southern Tien Shan[J]. *Lithos*, 97: 140–160.
- Konopelko D, Seltmann R, Biske G, Lepekhina E, Sergeev S. 2009. Possible source dichotomy of contemporaneous post–collisional barren I-type versus tin bearing A-type granites, lying on opposite sides of the South Tien Shan suture[J]. *Ore Geology Reviews*, 35, 206–216.
- Li Changmin. 2009. A review on the mineralogy and situ microanalytical dating techniques of Zircons[J]. *Geological Survey and Research*, 33(3): 161–174 (in Chinese with English abstract).
- Li Ping, Liu Hongxu, Ding Bo, Tian Mingming. 2018. The Zircon U–Pb geochronology and dynamics mechanism for the formation of monzonitic granite in the Qiongbola area, south of Yili basin[J]. *Geology in China*, 45(4): 720–739 (in Chinese with English abstract).
- Li Y J, Wang Z M, Wu H R, Huang Z B, Tan Z J, Luo J C. 2002. Discovery of Radiolarian fossils from the Aiketik group at the western end of South Tianshan Mountains of China and its

- implications[J]. *Acta Geologica Sinica*, 76(2): 146–154.
- Li Yuejun, Song Wenjie, Mai Guangrong, Zhou Lixia, Hu Jianfeng, Shang Xinlu. 2001. Characteristics of Kuqa and Northern Tarim Foreland basins and their coupling relation to South Tianshan orogeny[J]. *Xinjiang Petroleum Geology*, 22(5): 376–381 (in Chinese with English abstract).
- Li Yuejun, Sun Longde, Wu Haoruo, Wang Guolin, Yang Chaoshi, Peng Gengxin. 2005. Permo–Carboniferous radiolaria from the Wupatarkan Group, west terminal of Chinese South Tianshan[J]. *Chinese Journal of Geology*, 40(2): 220–226 (in Chinese with English abstract).
- Li Zhipei, Bai Jianke, Ru Yanjiao, Li Ting, Li Xiaoying. 2021. Age and petro–geochemistry of high–aluminum basalts from northern Zhaosu County of Xinjiang: The sign to convergent margins of Early Carboniferous plate in West Tianshan[J]. *Geological Bulletin of China*, 40(6): 864–879 (in Chinese with English abstract).
- Lin Tao, Deng Yufeng, Chen Bin, Wang Zhiqiang, Sun Keke, Zhao Bingbing. 2019. Geochronology, geochemistry and petrogenesis of the Kongwusayi A–type granites in the eastern Alataw Mountain, West Tianshan, Xinjiang[J]. *Acta Geologica Sinica*, 93(5): 1020–1036 (in Chinese with English abstract).
- Liu Benpei, Wang Ziqiang, Zhang Chuanheng. 1996. The Tectonic Framework and Evolution in Southwest Tianshan Mountains, China[M]. Wuhan: China University of Geosciences Press, 1–120 (in Chinese with English abstract).
- Liu Chuxiong, Xu Baoliang, Zhou Tianren, Lu Fengxiang, Tong Ying, Cai Jianhui. 2004. Petrochemistry and tectonic significance of Hercynian alkaline rocks along the northern margin of the Tarim platform and its adjacent area[J]. *Xinjiang Geology*, 22(1): 43–49 (in Chinese with English abstract).
- Liu Chunhua, Wu Cailai, Gao Yuanhong, Lei Min, Qin Haipeng, Li Mingze. 2014. Zircon LA–ICP–MS U–Pb dating and Lu–Hf isotopic system of A–type granitoids in South Tianshan, Baicheng County, Xinjiang. [J]. *Acta Petrologica Sinica*, 30(6): 1595–1614 (in Chinese with English abstract).
- Liu Guiping, Guo Ruiqing, Wei Zhen, Sun Minjia, Cui Tao, Wu Huanan, Song Zhihao. 2021. Geochemical characteristics and significance of the whole rock Sr–Nd and Zircon Hf isotopic in the Paleozoic Granite–plutons in Kuruktag, Xinjiang[J]. *Northwestern Geology*, 54(3): 39–50 (in Chinese with English abstract).
- Long L L, Cao J, Wang J B, Qian Q, Xiong X M, Wang Y W, Wang L J, Gao L M. 2008. Geochemistry and SHRIMP zircon U–Pb age of post–collisional granites in the Southwest Tianshan orogenic belt of China: Examples from the Heiyingshan and Laohutai plutons[J]. *Acta Geologica Sinica (English Edition)*, 82(2): 415–424.
- Ma Letian, Zhang Zhaochong, Dong Shuyun, Zhang Shu, Zhang Dongyang, Huang He. 2010. Geology and geochemistry of the Yingmailai Granitic Intrusion in the Southern Tianshan and its implications[J]. *Earth Science (Journal of China University of Geosciences)*, 35(6): 908–920 (in Chinese with English abstract).
- Ma X X, Shu L S, Meert J G. 2015. Early Permian slab breakoff in the Chinese Tianshan belt inferred from the post–collisional granitoids[J]. *Gondwana Research*, 27(1): 228–243.
- Maniar P D, Piccoli P M. 1989. Tectonic discrimination of granitoids[J]. *Geological Society of America Bulletin*, 101(5): 635–643.
- Mao Youliang, Fan Shuanghu, Chen Shue, Su Chunqian, Zhi Rongjun, Rui Ting, Wang Jiangwei, Liu Ming. 2014. Geochronology, petrogenesis and geological significance of the high–K calc–alkaline granites in the South Tianshan[J]. *Geological Journal of China Universities*, 20(1): 58–67 (in Chinese with English abstract).
- McKenzie D. 1989. Some remarks on the movement of small melt fractions in the mantle[J]. *Earth and Planetary Science Letters*, 95 (1/2): 53–71.
- Meng Linghua, Ma Mingyong, Cui Qinggang. 2022. LA–ICP–MS zircon U–Pb dating of the Wenquan pluton group in western Tianshan, Xinjiang and its geological significance[J]. *Geology and Exploration*, 58(3): 597–608 (in Chinese with English abstract).
- Pearce J A, Harris N B W, Tindle A G. 1984. Trace element discrimination diagrams for the tectonic interpretation of granitic rocks[J]. *Journal of Petrology*, 25(4): 956–983.
- Peccerillo R, Taylor S R. 1976. Geochemistry of Eocene calc–alkaline volcanic rocks from the Kastamonu area, northern Turkey[J]. *Contributions to Mineralogy and Petrology*, 58(1): 63–81.
- Pu Xiaofei, Song Shuguang, Zhang Lifei, Wei Chunjing. 2011. Silurian arc volcanic slices and their tectonic implications in the southwestern Tianshan UHPM belt, NW China[J]. *Acta Petrologica Sinica*, 27(6): 1675–1687 (in Chinese with English abstract).
- Qin Qie. 2017. Geochronology, petrogenesis and tectonic significances of the Paleozoic Intrusions in the Northern Margin of Tarim Craton and the South Tianshan[D]. Beijing: China University of Geosciences (Beijing), 1–162 (in Chinese with English abstract).
- Qin X, Chen X H, Shao Z G, Zhang Y P, Wang Y C. 2021. New timing of the Indosinian intracontinental deformation from the Triassic growth strata in the Kuqa Depression, Southern Tianshan, China[J]. *China Geology*, 4: 1–3.
- Simon L H, Nigel M K. 2007. Zircon: Tiny but timely[J]. *Elements*, 3 (1): 3–18.
- Solomovich L I, Trifonov B V. 2002. Postcollisional granites in the South Tian Shan Vairscan collisional belt, Kyrgyzstan[J]. *Journal of Asian Earth Sciences*, 21: 7–21.
- Spulber S D, Rutherford M J. 1983. The origin of rhyolite and plagiogranite in oceanic crust: An experimental study[J]. *Journal of Petrology*, 24(1): 1–25.
- Sun S S, McDonough W F. 1989. Chemical and isotopic systematics of oceanic basalts: implications for mantle composition and processes[C] //Saunders A D, Norry M J. *Magmatism in the Ocean*

- Basins. Geological Society, London: Special Publications, 42: 313–345.
- Su W, Cao J, Klemd R. 2010. U–Pb zircon geochronology of Tianshan eclogites in NW China: Implication for the collision between the Yili and Tarim blocks of the southwestern Altaids [J]. European Journal of Mineralogy, 22: 473–478.
- Taylor S R, McLennan S M. 1985. The continental crust: Its composition and evolution, an examination of the geochemical record preserved in Sedimentary Rocks [J]. Journal of Geology, 94 (4): 632–633.
- Turner S P, Foden J D, Morrison R S. 1992. Derivation of some A-type magmas by fractionation of basaltic magma: an example from the Padthaway Ridge, South Australia[J]. Lithos, 28(2): 151–179.
- Wang Chao, Liu Liang, Luo Jinhai, Che Zicheng, Teng Zhihong, Cao Xuanduo, Zhang Jingyi. 2007. Late Paleozoic post-collisional magmatism in the Southwestern Tianshan orogenic belt, take the Baleigong pluton in the Kokshal region as an example[J]. Acta Petrologica Sinica, 23(8): 1830–1840 (in Chinese with English abstract).
- Wang Qingtong, Wang Zhijun, Wang Haigen, Wang Lizhi, Liu Shibin, Zhang Xiaolei. 2021. Geochemical characteristics and geological significance of Permian Reef limestone in the Northwest of Tarim Basin[J]. Northwestern Geology, 54(4): 49–58 (in Chinese with English abstract).
- Wang Zongxiu, Li Chunlin, Pak Nikolai, Ivleva Elena, Yu Xinqi, Zhou Gaozhi, Xiao Weifeng, Han Shuqin, Halilov Zailabidin, Takenov Nurgazy, Yan Xili. 2017. Tectonic division and Paleozoic ocean-continent transition in Western Tianshan Orogen[J]. Geology in China, 44(4): 623–641 (in Chinese with English abstract).
- Waston E B, Harrison T M. 1983. Zircon saturation revisited: Temperature and composition effects in a variety of crustal magma A-types[J]. Earth and Planetary Science Letters, 64(2): 295–304.
- Whalen J B, Currie K L, Chappell B W. 1987. A-type granites: Geochemical characteristics discrimination and petrogenesis[J]. Contributions to Mineralogy and Petrology, 95: 407–419.
- Wu C, Hong T, Xu X W, Wang C X, Dong L H. 2021. Report of 2.7 Ga zircon U–Pb age of orthogneiss in the Wenquan metamorphic complex, West Tianshan, China[J]. China Geology, 4: 1–4.
- Wu Yuanbao, Zheng Yongfei. 2004. Study on the zircon geneticmineralogy and its constraint to U–Pb age interpretation[J]. Chinese Science Bulletin, 49(16): 1589–1604 (in Chinese with English abstract).
- Xia Linqi, Xia Zuchun, Xu Xueyi, Li Xiangmin, Ma Zhongping, WangLishe. 2004. Carboniferous Tianshan igneous megaprovince and mantle plume[J]. Geological Bulletin of China, 23(9/10): 903–910 (in Chinese with English abstract).
- Xia Linqi, Zhang Guowei, Xia Zuchun, Xu Xueyi, Dong Yunpeng, Li Xiangmin. 2002. Constraints on the timing of opening and closing of the Tianshan Paleozoic oceanic basin: Evidence from Sinian and Carboniferous volcanic rocks[J]. Geological Bulletin of China, 21 (2): 55–62 (in Chinese with English abstract).
- Xiao W J, Li S Z, Santosh M. 2012. Orogenic belts in Central Asia: Correlations and connections[J]. Journal of Asian Earth Sciences, 49: 1–6.
- Xiao W J, Windley B F, Allen M B. 2013. Paleozoic multiple accretionary and collisional tectonics of the Chinese Tianshan orogenic collage[J]. Gondwana Research, 23: 1316–1341.
- Xu Xueyi, Ma Zhongping, Xia Zuchun, Xia Linqi, Li Xiangmin, Wang Lishe. 2005. Discussion of the sources and characteristics on Sr, Nd, Pb isotopes of the Carboniferous to Permian post-collision granites from Tianshan[J]. Northwestern Geology, 38(2): 1–18 (in Chinese with English abstract).
- Yang Gaoxue, Li Yongjun, Zhang Bing, Wang Yabing, Liu Zhenwei, Yan Jing, Tian Zhixian. 2013. Geochronology, geochemistry and petrogenesis of the Jietebutiao A-type granites in West Junggar, Xinjiang[J]. Acta Geoscientia Sinica, 34(3): 295–306 (in Chinese with English abstract).
- Yang Rong. 2016. The Study of Magma Mixing in Late Paleozoic of Borohuoro in the West Tianshan Orogeny[D]. Xi'an: Northwest University, 1–89 (in Chinese with English abstract).
- Yu Jiyuan, Ji Bo, Wang Guoqiang. 2018. Geochemistry of dioritic enclaves related to magmatic mixing in the concentrically zoned Alatake igneous complex, central Tianshan Mountains[J]. Geology in China, 45(4): 767–782 (in Chinese with English abstract).
- Zhang C L, Zou H. 2013. Permian A-type granites in Tarim and western part of Central Asian Orogenic Belt (CAOB): Genetically related to a common Permian mantle plume?[J]. Lithos, 172–173: 47–60.
- Zhang L F, Ai Y L, Li X P, Rubatto D, Song B, Williams S, Song S G, Ellis D, Liou J G. 2007. Triassic collision of western Tianshan orogenic belt, China: Evidence from SHRIMP U–Pb dating of zircon from HP/UHP eclogitic rocks[J]. Lithos, 96(1/2): 266–280.
- Zhang Lifei, Ai Yongliang, Li Qiang, Li Xuping, Song Shuguang, Wei Chunjing. 2005. The formation and tectonic evolution of UHP metamorphic belt in southwestern Tianshan, Xinjiang[J]. Acta Petrologica Sinica, 21(4): 1029–1038 (in Chinese with English abstract).
- Zhang Qi, Pan Guoqiang, Li Chengdong, Jin Weijun, Jia Xiuqin. 2007. Does fractional crystallization occur in granitic magma? Some crucial questions on granite study[J]. Acta Petrologica Sinica, 23 (6): 1239–1251 (in Chinese with English abstract).
- Zhang Qi, Ran Hao, Li Chengdong. 2012. A-type granite: What is the essence?[J]. Acta Petrologica et Mineralogica, 31(4): 621–626 (in Chinese with English abstract).
- Zhang Zhaochong, Dong Shuyun, Huang He, Ma Letian, Zhang Dongyang, Zhang Shu, Xue Chunji. 2009. Geology and geochemistry of the Permian intermediate acid intrusions in the southwestern Tianshan, Xinjiang, China: Implications for

- petrogenesis and tectonics[J]. Geological Bulletin of China, 28(12): 1827–1839 (in Chinese with English abstract).
- Zhao Chuang, Su Xuliang, Xue Bin, Cheng Dongjiang, Shi Xingjun, Song Taotao, Zhang Kuo. 2021. Zircon U–Pb dating and geochemical characteristics of the granites in Kuchuwula–Yingba area of western Inner Mongolia[J]. Geology in China, 48(1): 189–206 (in Chinese with English abstract).
- Zhao Yayun, Liu Xiaofeng, Yang Chunsi, Zhang Xiaoqiang, Liu Yuanchao, Zheng Changyun, Gong Fuzhi, Hua Kang. 2022. Recognition of A-type granite and its implication for magmatism and mineralization in Tangge skarn-type Cu-polymetallic deposit, Tibet[J]. Geology in China, 49(2): 496–517 (in Chinese with English abstract).
- Zhao Zhenhua, Bai Zhenghua, Xiong Xiaolin, Mei Houjun, Wang Yixian. 2003. $^{40}\text{Ar}/^{39}\text{Ar}$ chronological study of Late Paleozoic volcanic–hypabyssal igneous rocks in western Tianshan, Xinjiang[J]. Geochimica, 32(4): 317–327 (in Chinese with English abstract).
- Zhou Zhenju, Chen Zhingle, Zhang Wengao, Zhang Tao, Zhang Qing, Han Fengbin, Huo Hailong, Yang Bin, Ma Ji, Wang Wei, Wang Cheng, Liu Xianjun. 2022. Structural deformation and fluid evolution associated with the formation of the Sawayardun gold deposit in Southwestern Tianshan Orogen[J]. Geology in China, 49(1): 181–200 (in Chinese with English abstract).
- Zhou Zongliang, Gao Shuhai, Liu Zhizhong. 1999. West–south Tianshan mountain orogenic belt and foreland basin systems[J]. Geoscience, 13(3): 275–280 (in Chinese with English abstract).
- Zhu Yongfen, Zhang Lifei, Gu Libing, Cuo Xuan, Zhou Jing. 2005. SHRIMP geochronology and geochemistry of Carboniferous volcanic rocks in the western Tianshan area[J]. Chinese Science Bulletin, 50(18): 2004–2014 (in Chinese with English abstract).
- Zhu Zhixing, Li Jinyi, Dong Lianhui, Zhang Xiaofan, Hu Jianwei, Wang Kezhuo. 2008. The age determination of Late Carboniferous intrusions in Mangqisi region and its constraints to the closure of oceanic basin in South Tianshan, Xinjiang[J]. Acta Petrologica Sinica, 24(12): 2761–2766 (in Chinese with English abstract).
- Zorpi M J, Coulon C, Orsini J B. 1989. Magma mingling, zoning and emplacement in calc–alkaline granitoid plutons[J]. Tectonophysics, 157(4): 315–329.
- ### 中文参考文献
- 蔡东升, 卢华夏, 贾东, 吴世敏. 1995. 南天山古生代板块构造演化[J]. 地质论评, 41(5): 432–443.
- 陈加杰, 付乐兵, 魏俊浩, 田宁, 熊乐, 赵玉京, 张玉洁, 郑月清. 2016. 东昆仑沟里地区晚奥陶世花岗闪长岩地球化学特征及其对原特提斯洋演化的制约[J]. 地球科学, 41(11): 1863–1882.
- 陈士海, 钟文, 张健仁. 2020. 新疆南天山景汗花岗岩体年代学、地
球化学特征及其构造意义[J]. 华东地质, 41(2): 128–141.
- 高俊, 龙灵利, 钱青, 黄德志, 苏文, Klemd R. 2006. 南天山: 晚古生代还是三叠纪碰撞造山带?[J]. 岩石学报, 22(5): 1049–1061.
- 耿全如, 李文昌, 王立全, 曾祥婷, 彭智敏, 张向飞, 张璋, 丛峰, 关俊雷. 2021. 特提斯中西段古生代洋陆格局与构造演化[J]. 沉积与特提斯地质, 41(2): 297–315.
- 郝国杰, 王惠初, 牛广华, 康健丽, 郝爽. 2020. 中国变质大地构造研究及科学意义[J]. 地质调查与研究, 43(2): 89–96.
- 黄岗, 张占武, 董志辉, 张文峰. 2011. 南天山铜花山蛇绿混杂岩中斜长花岗岩锆石LA-ICP-MS微区U-Pb定年及其地质意义[J]. 中国地质, 38(1): 94–102.
- 黄河, 王涛, 秦切, 童英, 郭磊, 张磊, 候继尧, 宋鹏. 2015. 南天山西段巴雷公花岗岩体的地质年代学及锆石Hf同位素特征——岩石成因及对构造演化的约束[J]. 岩石矿物学杂志, 34(6): 971–990.
- 黄河, 张东阳, 张招崇, 张舒, 李宏波, 薛春纪. 2010. 南天山川乌鲁碱性杂岩体的岩石学和地球化学特征及其岩石成因[J]. 岩石学报, 26(3): 947–962.
- 黄河, 张招崇, 张东阳, 杜红星, 马乐天, 康建丽, 薛春纪. 2011. 中国南天山晚石炭世—早二叠世花岗质侵入岩的岩石成因与地壳增生[J]. 地质学报, 85(8): 1305–1333.
- 计文化, 李荣社, 陈奋宁, 杨博. 2020. 中国西北地区南华纪—古生代构造重建及关键问题讨论[J]. 地质力学学报, 26(5): 634–655.
- 贾乘造. 1997. 中国塔里木盆地构造特征与油气[M]. 北京: 石油工业出版社: 1–295.
- 姜雪薇, 吕增. 2021. 西南天山变质俯冲杂岩带的内部结构——来自木扎尔特剖面的启示[J]. 岩石矿物学杂志, 40(6): 1181–1187.
- 李长民. 2009. 锆石成因矿物学与锆石微区定年综述[J]. 地质调查与研究, 33(3): 161–174.
- 李平, 刘红旭, 丁波, 田明明. 2018. 伊犁盆地南缘琼博拉二长花岗岩锆石U-Pb年代学及形成功力学机制[J]. 中国地质, 45(4): 720–739.
- 李曰俊, 宋文杰, 买光荣, 周黎霞, 胡剑风, 尚新路. 2001. 库车和北塔里木前陆盆地与南天山造山带的耦合关系[J]. 新疆石油地质, 22(5): 376–381.
- 李曰俊, 孙龙德, 吴浩若, 王国林, 杨朝世, 彭更新. 2005. 南天山西端乌帕塔尔坎群发现石炭一二叠纪放射虫化石[J]. 地质科学, 40(2): 220–226.
- 李智佩, 白建科, 茹艳娇, 李婷, 李晓英. 2021. 新疆昭苏县北高铝玄武岩时代、岩石学和地球化学特征——西天山早石炭世汇聚板块构造的标志[J]. 地质通报, 40(6): 864–879.
- 林涛, 邓宇峰, 陈斌, 王志强, 孙克克, 赵冰冰. 2019. 新疆西天山阿拉套山东部孔吾萨依A型花岗岩成岩年代、地球化学特征及成因[J]. 地质学报, 93(5): 1020–1036.
- 刘本培, 王自强, 张传恒. 1996. 西南天山构造格局与演化[M]. 武汉: 中国地质大学出版社, 1–120.
- 刘楚雄, 许保良, 邹天人, 路凤香, 童英, 蔡剑辉. 2004. 塔里木北缘及邻区海西期碱性岩岩石学特征及其大地构造意义[J]. 新疆地

- 质, 22(1): 43–49.
- 刘春花, 吴才来, 郜源红, 雷敏, 秦海鹏, 李名则. 2014. 南天山拜城县波孜果尔A型花岗岩类锆石U-Pb定年及其Lu-Hf同位素组成[J]. 岩石学报, 30(6): 1595–1614.
- 刘桂萍, 郭瑞清, 魏震, 孙敏佳, 崔涛, 吴华楠, 宋志豪. 2021. 新疆库鲁克塔格地区古生代花岗岩侵入岩全岩Sr-Nd和锆石Hf同位素地球化学特征及其意义[J]. 西北地质, 54(3): 39–50.
- 马乐天, 张招崇, 董书云, 张舒, 张东阳, 黄河. 2010. 南天山英买来花岗岩的地质、地球化学特征及其地质意义[J]. 地球科学(中国地质大学学报), 35(6): 908–920.
- 毛友亮, 樊双虎, 陈淑娥, 苏春乾, 职荣军, 芮婷, 王江伟, 刘明. 2014. 南天山高钾钙碱性花岗岩年代学、岩石成因及其地质意义[J]. 高校地质学报, 20(1): 58–67.
- 孟令华, 马明永, 崔庆岗. 2022. 新疆西天山温泉岩体群LA-ICP-MS锆石U-Pb定年及其地质意义[J]. 地质与勘探, 58(3): 597–608.
- 蒲晓菲, 宋述光, 张立飞, 魏春景. 2011. 西南天山超高压变质带中志留纪岛弧火山岩岩片及其构造意义[J]. 岩石学报, 27(6): 1675–1687.
- 秦切. 2017. 塔里木北缘—南天山地区古生代侵入岩年代学、成因及构造意义[D]. 北京: 中国地质大学(北京), 1–162.
- 王超, 刘良, 罗金海, 车自成, 滕志宏, 曹宣铎, 张静艺. 2007. 西南天山晚古生代后碰撞岩浆作用: 以阔克萨彦岭地区巴雷公花岗岩为例[J]. 岩石学报, 23(8): 1830–1840.
- 王庆同, 王志军, 王海根, 王立志, 刘世彬, 张晓磊. 2021. 塔里木盆地西北缘二叠纪生物礁灰岩地球化学特征及其地质意义[J]. 西北地质, 54(4): 49–58.
- 王宗秀, 李春麟, Pak Nikolai, Ivleva Elena, 余心起, 周高誌, 肖伟峰, 韩淑琴, Halilov Zailabidin, Takenov Nurgazy, 鄭犀利. 2017. 西天山造山带构造单元划分及古生代洋陆转换过程[J]. 中国地质, 44(4): 623–641.
- 吴元保, 郑永飞. 2004. 锆石成因矿物学研究及其对U-Pb年龄解释的制约[J]. 科学通报, 49(16): 1589–1604.
- 夏林圻, 夏祖春, 徐学义, 李向民, 马中平, 王立社. 2004. 天山石炭纪大火成岩省与地幔柱[J]. 地质通报, 23(9/10): 903–910.
- 夏林圻, 张国伟, 夏祖春, 徐学义, 董云鹏, 李向民. 2002. 天山古生代洋盆开启、闭合时限的岩石约束——来自震旦纪、石炭纪火山岩的证据[J]. 地质通报, 21(2): 55–62.
- 徐学义, 马中平, 夏祖春, 夏林圻, 李向民, 王立社. 2005. 天山石炭—二叠纪后碰撞花岗岩的Nd、Sr、Pb同位素源区示踪[J]. 西北地质, 38(2): 1–18.
- 杨高学, 李永军, 张兵, 汪雅兵, 刘振伟, 严镜, 田陟贤. 2013. 新疆西准噶尔接特布调A型花岗岩年代学、地球化学及岩石成因[J]. 地球学报, 34(3): 295–306.
- 杨蓉. 2016. 西天山博罗科努地区晚古生代岩浆混合作用研究[D]. 西安: 西北大学, 1–89.
- 余吉远, 计波, 王国强. 2018. 中天山阿拉塔格环状杂岩体中闪长质包体地球化学与岩浆混合作用[J]. 中国地质, 45(4): 767–782.
- 张立飞, 艾永亮, 李强, 李旭平, 宋述光, 魏春景. 2005. 新疆西南天山超高压变质带的形成与演化[J]. 岩石学报, 21(4): 1029–1038.
- 张旗, 潘国强, 李承东, 金惟俊, 贾秀勤. 2007. 花岗岩结晶分离作用问题——关于花岗岩研究的思考之二[J]. 岩石学报, 23(6): 1239–1251.
- 张旗, 冉皞, 李承东. 2012. A型花岗岩的实质是什么?[J]. 岩石矿物学杂志, 31(4): 621–626.
- 张招崇, 董书云, 黄河, 马乐天, 张东阳, 张舒, 薛春纪. 2009. 西南天山二叠纪中酸性侵入岩的地质学和地球化学: 岩石成因和构造背景[J]. 地质通报, 28(12): 1827–1839.
- 赵闯, 苏旭亮, 薛斌, 程东江, 史兴俊, 宋涛涛, 张阔. 2021. 内蒙古西部苦楚乌拉—英巴地区花岗岩锆石U-Pb定年及地球化学特征[J]. 中国地质, 48(1): 189–206.
- 赵亚云, 刘晓峰, 杨春四, 张小强, 刘远超, 郑常云, 龚福志, 华康. 2022. 西藏唐格砂卡岩型铜多金属矿床A型花岗岩的识别及其对成岩成矿的指示[J]. 中国地质, 49(2): 496–517.
- 赵振华, 白正华, 熊小林, 梅厚钧, 王一先. 2003. 西天山北部晚古生代火山—浅侵位岩浆岩⁴⁰Ar/³⁹Ar同位素定年[J]. 地球化学, 32(4): 317–327.
- 周振菊, 陈正乐, 张文高, 张涛, 张青, 韩凤彬, 霍海龙, 杨斌, 马骥, 王威, 王成, 柳献军. 2022. 西南天山萨瓦亚尔顿金矿床构造—流体控矿作用研究[J]. 中国地质, 49(1): 181–200.
- 周宗良, 高树海, 刘志忠. 1999. 西南天山造山带与前陆盆地系统[J]. 现代地质, 13(3): 275–280.
- 朱永峰, 张立飞, 古丽冰, 郭璇, 周晶. 2005. 西天山石炭纪火山岩SHRIMP年代学及其微量元素地球化学研究[J]. 科学通报, 50(18): 2004–2014.
- 朱志新, 李锦轶, 董连慧, 张晓帆, 胡建卫, 王克卓. 2008. 新疆南天山盲起苏晚石炭世侵入岩的确定及对南天山洋盆闭合时限的限定[J]. 岩石学报, 24(12): 2761–2766.